

STREAM NITROGEN UPTAKE DYNAMICS FROM AMBIENT TO
SATURATION ACROSS DEVELOPMENT GRADIENTS,
STREAM NETWORK POSITION, AND SEASONS

by

Rebecca Anne McNamara

A thesis submitted in partial fulfillment
of the requirements for the degree

of

Master of Science

in

Land Resources and Environmental Sciences

MONTANA STATE UNIVERSITY
Bozeman, Montana

July 2010

©COPYRIGHT

by

Rebecca Anne McNamara

2010

All Rights Reserved

APPROVAL

of a thesis submitted by

Rebecca Anne McNamara

This thesis has been read by each member of the thesis committee and has been found to be satisfactory regarding content, English usage, format, citation, bibliographic style, and consistency, and is ready for submission to the Division of Graduate Education.

Dr. Brian L. McGlynn

Approved for the Department of Land Resources and Environmental Sciences

Dr. Tracy M. Sterling

Approved for the Division of Graduate Education

Dr. Carl A. Fox

STATEMENT OF PERMISSION TO USE

In presenting this thesis in partial fulfillment of the requirements for a master's degree at Montana State University, I agree that the Library shall make it available to borrowers under rules of the Library.

If I have indicated my intention to copyright this thesis by including a copyright notice page, copying is allowable only for scholarly purposes, consistent with "fair use" as prescribed in the U.S. Copyright Law. Requests for permission for extended quotation from or reproduction of this thesis in whole or in parts may be granted only by the copyright holder.

Rebecca Anne McNamara

July 2010

ACKNOWLEDGEMENTS

I would like to offer many thanks to my committee chair, Dr. Brian McGlynn, for endless hours of consultation within which he extended guidance, insight, and intellectual stimulation. Brian has been extremely motivating and supportive, and my time spent working with him has been an excellent educational and personal experience. I would like to thank my committee members Dr. Lucy Marshall and Dr. Wyatt Cross. Their comments, guidance, and encouragement have been very helpful and have greatly improved the quality of this thesis. I would also like to thank past and present members of the Watershed Hydrology Lab at Montana State University, Kristin Harder, Tim Covino, Galena Montross, Diego Riveros-Iregui, Kelsey Jencso, Vince Pacific, and John Mallard for their field and lab assistance, motivation, discussions, and above all, friendship. I want to further thank Tim Covino for many hours of conversation and guidance with data analysis and writing as well as Kristin Harder for assistance with the background investigation. I extend my gratitude to field assistants Trish Jenkins and Kelley Conde whose hard work was steadfast. I thank Galena Montross and John Mallard for many hours of lab work. Thanks to friends from other disciplines for support outside of academia. I extend my utmost gratitude to Jake Beam for unwavering support during the final year and a half of my thesis work. Finally, I would like to thank my parents, Mike and Anne McNamara, and my brothers, Ted and Charlie as well as their families, for their love, support, and encouragement. My Master's thesis project has been an amazing experience that has expanded both my educational and personal erudition.

TABLE OF CONTENTS

| | |
|--|----|
| 1. INTRODUCTION | 1 |
| Historical Context and Scientific Background | 1 |
| Study Area | 3 |
| Purpose..... | 5 |
| References Cited..... | 6 |
| 2. STREAM NITROGEN UPTAKE DYNAMICS FROM AMBIENT TO SATURATION ACROSS DEVELOPMENT GRADIENTS, STREAM NETWORK POSITION, AND SEASONS | 10 |
| Introduction..... | 10 |
| Methods..... | 15 |
| Study Area | 14 |
| Experimental Design..... | 16 |
| Stream Discharge | 18 |
| Stream Tracer Experiments using Constant-rate Additions of Cl and NO ₃ -N | 18 |
| Field Methods and Chemical Analysis | 18 |
| Calculating NO ₃ -N Spiraling Parameters using the Plateau Approach | 20 |
| Stream Tracer Experiments using Instantaneous Slug Additions of Cl and NO ₃ -N | 21 |
| Field Methods and Chemical Analysis | 21 |
| Mass Recovery of Cl and NO ₃ -N..... | 22 |
| Calculating Breakthrough Curve-integrated Stream NO ₃ -N Concentration..... | 23 |
| Calculating Stream NO ₃ -N Uptake Dynamics through BTC-integration | 24 |
| Calculating Stream NO ₃ -N Uptake Dynamics using the TASCC Method..... | 25 |
| Ambient and Total NO ₃ -N Uptake Dynamics and Kinetic Model Parameters..... | 26 |
| Calculating Ambient Stream NO ₃ -N Uptake Parameters | 26 |
| Calculating Total Stream NO ₃ -N Concentrations Associated with Tracer Addition Experiments..... | 26 |
| Calculating Stream Total NO ₃ -N Uptake Parameters..... | 27 |
| Calculating Maximum Areal Uptake Rate and Half-Saturation Constant using the Michaelis-Menten Kinetic Model | 28 |

TABLE OF CONTENTS – CONTINUED

| | |
|--|----|
| Results..... | 29 |
| Variability in Measured Stream Discharge across Experimental Reaches..... | 29 |
| Physical and Biological Retention of Added NO ₃ -N..... | 29 |
| Ambient Uptake Dynamics..... | 30 |
| NO ₃ -N Spiraling Parameters from Constant-rate Additions (Plateau Approach)..... | 32 |
| NO ₃ -N Spiraling Parameters Calculated through BTC-integration..... | 33 |
| Total NO ₃ -N Uptake Parameters and M-M kinetics..... | 34 |
| Seasonal Variation in NO ₃ -N Retention and Uptake Dynamics..... | 36 |
| Results Summary..... | 38 |
| Discussion..... | 40 |
| How do Stream Uptake Kinetics and Spiraling Parameters Vary across Streams of Different Development Intensity and Scale?..... | 40 |
| Assessment of Watershed Size (Watershed Area and Discharge) and Nitrate Concentration on Influences on Uptake Kinetics..... | 40 |
| Assessment of Uptake Kinetic Model Shapes..... | 47 |
| How do Uptake Kinetics and Spiraling Parameters Vary across Season in a Snow Dominated Mountain Stream?..... | 48 |
| What are the Relative Magnitudes of Stream Physical versus Biologic Retention of Added Nitrate across Streams from 1 st to 4 th Order?..... | 52 |
| Summary..... | 55 |
| References Cited..... | 58 |
| 3. SUMMARY..... | 82 |
| References Cited..... | 85 |

LIST OF TABLES

| Table | Page |
|--|------|
| 1. Location, reach characteristics and season of tracer addition experiments conducted in the West Fork Gallatin Watershed | 64 |
| 2. Dates when tracer addition experiments were conducted, physical characteristics, ambient NO ₃ -N concentrations for the day of the experiment and average annual NO ₃ -N concentrations for the six experimental stream reaches | 65 |
| 3. Total, physical, and biological NO ₃ -N retention for each instantaneous tracer addition | 66 |
| 4. Ambient uptake parameters including ambient uptake length (S_{w-amb}), ambient uptake velocity (V_{f-amb}), ambient areal uptake rate (U_{amb}), and Michaelis-Menten (M-M) uptake parameters (U_{max} and K_m) for each tracer addition experiment | 67 |
| 5. Uptake dynamics for constant-rate tracer addition experiments..... | 68 |
| 6. Breakthrough curve (BTC) integrated uptake dynamics for instantaneous tracer addition experiments..... | 69 |

LIST OF FIGURES

| Figure | Page |
|---|------|
| 1.1: (A) Map of Montana showing the location of the West Fork Gallatin Watershed, and (B) shows location of each of the six experimental stream reach within the watershed..... | 8 |
| 1.2: Time series of the number of structures and average annual ambient NO ₃ -N concentrations over the last forty years in the West Fork Gallatin Watershed..... | 9 |
| 2.1: (A) Map of Montana showing the location of the West Fork Gallatin Watershed, and (B) shows location of each of the six experimental stream reach within the watershed..... | 70 |
| 2.2: Time series of the number of structures and average annual ambient NO ₃ -N concentrations over the last forty years in the West Fork Gallatin Watershed..... | 71 |
| 2.3: Conceptual model describing how to calculate uptake length (S_w) and areal uptake rate (U) from NO ₃ -N and Cl concentrations measured during the experimental breakthrough curve (BTC)..... | 72 |
| 2.4: (A) Physical and (B) biological NO ₃ -N retention for five of six stream reaches versus their watershed areas. (C) The ratio of biologic to total NO ₃ -N retention versus watershed area. (D) Biologic NO ₃ -N retention versus physical NO ₃ -N retention | 73 |
| 2.5: (A) Ambient uptake length (S_{w-amb}) and (B) ambient uptake velocity (V_{f-amb}) for the six stream reaches versus ambient NO ₃ -N concentrations for the day of the experiment (open symbols). (C) Ambient uptake length (S_{w-amb}) and (D) ambient uptake velocity (V_{f-amb}) for the six stream reaches versus average annual NO ₃ -N concentrations (solid symbols) | 74 |
| 2.6: (A-E) Ambient areal uptake rate (U_{amb}), (F-J) maximum areal uptake rate (U_{max}), and (K-O) half-saturation constant (K_m), versus watershed area (WA), stream order, discharge (Q), number of structures, and NO ₃ -N concentrations [NO ₃ -N] (ambient for the day of the experiment (solid symbols) and average annual (open symbols))..... | 75 |

LIST OF FIGURES – CONTINUED

| Figure | Page |
|--|------|
| 2.7: Total areal uptake rates of added nutrient plotted against total NO ₃ -N concentration for six stream reaches..... | 76 |
| 2.8: Michaelis-Menten (M-M) hyperbolic equation fits for total areal uptake rates for each grab sample calculated using the dynamic TASC approach ($U_{\text{tot-dyn}}$) versus total dynamic NO ₃ -N concentration..... | 77 |
| 2.9: Total dynamic uptake velocities ($V_{\text{f-tot-dyn}}$) for each grab sample versus total dynamic NO ₃ -N concentration [NO ₃ -N _{tot-dyn}] for the six stream reaches (A). (B) For five of the six sites, the hyperbolic decay models for each data set are presented | 78 |
| 2.10: (A-C) Five tracer addition experiments were conducted in Beehive from fall 2006 to winter 2009. The same reach was used for each experiment..... | 79 |
| 2.11: Total areal uptake rates versus total NO ₃ -N concentrations in the Beehive experimental stream reach for five seasons | 80 |
| 2.12: Total dynamic uptake velocities ($V_{\text{f-tot-dyn}}$) for each grab sample versus total dynamic NO ₃ -N concentration [NO ₃ -N _{tot-dyn}] for the five seasonal experiments in Beehive..... | 81 |

ABSTRACT

The balance between stream nitrogen (N) loading and retention determines stream network nutrient export dynamics. Nutrient retention can be altered due to changes in hydrology, nutrient loading, and biological community response to increased nutrient availability. We quantified physical and biological contributions to total nutrient retention and determined biological uptake kinetics from ambient to saturation across six stream reaches across the West Fork Gallatin Watershed (a 1st to 4th order, headwater, 240 km² watershed) which has experienced rapid exurban, resort development leading to increased watershed nutrient loading over the last four decades. We conducted 17 stream tracer experiments (constant-rate and instantaneous additions) using both conservative (chloride (Cl)) and biologically active (nitrate (NO₃-N)) tracers across a range of watershed areas (WA), stream discharges, seasons, development intensities, and ambient NO₃-N concentrations, reflecting varying degrees of development and upland nutrient loading (i.e., wastewater effluent). Ambient uptake (U_{amb}) was calculated and Michaelis–Menten kinetic models were used to quantify maximum areal uptake rates (U_{max}) and half-saturation constants (K_m) for each experimental reach. In the West Fork Gallatin Watershed, the majority of added NO₃-N was physically retained within stream reaches of smaller WA with decreasing physical retention as WA increased. However, as WA increased, biological retention of added NO₃-N became increasingly important and exceeded physical retention in the two largest watersheds. Further, U_{amb} and U_{max} values increased with greater WA, and U_{max} was greatest in the summer and lowest in the winter. Our results demonstrated that nutrient uptake variability between stream reaches was related to WA, discharge, ambient NO₃-N concentration, and season. Although some streams in the watershed no longer appear to be functioning at pre-development levels, none demonstrated saturation with respect to NO₃-N, yet with continued development and increased loading, nutrient saturation could occur. We suggest that quantifying physical and biological contributions to total retention and determining uptake kinetics from ambient to saturation over space, time, and development intensities can yield new insight into the capacity of stream networks to buffer nutrient loading.

CHAPTER 1

INTRODUCTION

Historical Context and Scientific Background

In the 1970s, the West Fork Gallatin Watershed was the focus of a research initiative conducted by the National Science Foundation RANN (Research Applied to National Needs) (National Science Foundation 1976). This research informs our study by providing background watershed characteristics and conditions prior to resort development. Since the RANN study was conducted, the number of structures within the watershed has grown from less than one hundred to more than 2500 and four ski resorts (both Alpine and Nordic), three golf courses and many other recreational opportunities have been developed. One of the primary concerns created by increased development is elevated nutrient loading to water bodies. With the increase in development over the last 40 years, average annual nitrate levels in the West Fork Gallatin River have increased an order of magnitude ($\sim 30 \mu\text{g l}^{-1} \text{NO}_3\text{-N}$ in 1971 to $\sim 300 \mu\text{g l}^{-1} \text{NO}_3\text{-N}$ in 2007) (Figure 1.2).

These increases in nitrogen concentrations as well as other nutrients and sediment have resulted in three streams in the West Fork Gallatin Watershed being placed on the State of Montana's 2002 list of impaired water (303d): the West Fork Gallatin River and two of its tributaries (headwaters of the Mississippi River) (Montana Department of Environmental Quality 2002). A snow dominated watershed in Colorado has experienced similar increases in nutrient loading due to resort development (Kaushal et

al. 2006). Headwater streams play an important role in riverine nutrient retention and downstream transport (Peterson et al. 2001).

The concerns for increases in nutrient loading go beyond the local scale, with nitrate being exported from headwaters streams downstream to larger river, reservoir, and coastal ecosystems, including potential further increases in nitrate delivered to the Gulf of Mexico, potentially creating a larger hypoxic zone (Galloway et al. 2004, Rabalais et al. 2010). To better understand the effects of nutrient transport from headwater systems, the concept of nutrient spiraling can be utilized and experiments conducted to determine stream uptake parameters.

The concept of nutrient spiraling was introduced in the late 1970s (Webster and Patten 1979, Newbold et al. 1981) and made popular through the development of the Stream Solute Workshop (1990). The nutrient spiraling concept is used to estimate the distance for which a nutrient molecule remains suspended in a water column before being utilized. Shorter spiraling lengths (S_w) indicate less time that the nutrient has been suspended in the water column or that the nutrient has been recycled frequently. Nutrient spiraling lengths are influenced by both physical (i.e., changes in discharge) (e.g., Valett et al. 1996, Butturini and Sabater 1998) and biological (i.e., changes in nutrient concentration) factors (e.g., Mulholland et al. 2008). Spiraling lengths are often converted to uptake efficiencies (V_f) or areal uptake rates (U) to account for the physical factors (i.e., discharge, velocity, stream bed area, depth, etc.) (Stream Solute Workshop 1990, Davis and Minshall 1999, Dodds et al. 2002).

In the second chapter of this thesis, I utilize the stream spiraling concept to assess the relative influences of physical and biologic nutrient retention mechanisms and biological uptake kinetics to assess how nitrate retention and uptake varies on a watershed or stream network scale, how the effects differ within a watershed that has varying development gradients, and how seasonality affects nitrogen retention in snow dominated mountain environments.

Study Area

This research was conducted in the West Fork Gallatin Watershed in the Madison Mountain Range of the Northern Rocky Mountains in Southwestern Montana, USA (Figure 1.1). Seventeen tracer addition experiments were conducted at six sites throughout the watershed. The six experimental stream reaches varied in watershed area (WA), stream discharge (Q), stream order, number of structures (including residential and commercial), ambient $\text{NO}_3\text{-N}$ concentrations [$\text{NO}_3\text{-N}_{amb}$], and average annual $\text{NO}_3\text{-N}$ concentrations (Tables 1 and 2 and Figure 1.1).

The West Fork Gallatin Watershed (240 km^2) contains three main subwatersheds: the South Fork Gallatin (121 km^2), the Middle Fork Gallatin (48 km^2), and the North Fork Gallatin (24 km^2) with the primary streams flowing from west to east. The elevation ranges from 1800 to 3400 m with well-defined steep topography and shallow soils. Dominant geology in the West Fork Gallatin Watershed varies from colluvium and glacial deposits in the valley bottoms to sedimentary (e.g. gravel deposits) and metasedimentary (e.g. granitic gneiss) formations of various ages and metamorphosed

volcanics of Archean age in the higher elevations. Precipitation ranges annually from less than 50 cm at low elevations to more than 127 cm at high elevations with the majority of precipitation falling as snow during the winter and spring months (Lone Mountain NRCS SNOTEL #590, 2707 m elevation). The growing season is short with 75-90 frost free days (fewer frost free days with increased elevation) from mid-June to mid-September (U.S. Department of Agriculture 1994). Vegetation in the higher elevations of the watershed is predominantly coniferous forest (Lodgepole pine (*Pinus contorta*), Blue spruce (*Picea pungens*), Engelmann spruce (*Picea engelmannii*) and Douglas-fir (*Pseudotsuga menziesii*)) and native grasses with willows (*Salix spp.*) and aspen (*Populus tremuloides*) groves in the riparian areas. Vegetation in the lower elevations is similar but is predominantly native grasses, shrubs and willows (*Salix spp.*) with fewer coniferous trees.

Seventeen stream tracer addition experiments were conducted throughout the watershed in six stream reaches (Figure 1.1 and Table 1). The six experimental stream reaches were: Pony, Beehive, Upper Middle Fork, North Fork, Lower Middle Fork and West Fork. Pony, Beehive, Upper Middle Fork, and Lower Middle Fork are located in the Middle Fork Gallatin Watershed. North Fork is located in the North Fork Gallatin Watershed. The final stream reach, West Fork, extends from the West Fork Gallatin's confluence with the Gallatin River to approximately 1100 meters upstream of the confluence (Figure 1.1). Please see tables 1 and 2 for additional information on the six stream reaches, their corresponding characteristics, and the season in which experiments

occurred. Nitrogen uptake and spiraling metric dynamics were determined from data collected during the tracer addition experiments.

Purpose

The purpose of this study was to investigate nitrate retention and uptake kinetics from ambient to saturation across the West Fork Gallatin Watershed. I present three main research questions:

- (1) How do stream uptake kinetics and spiraling parameters vary across streams of different development intensity and scale?
- (2) How do uptake kinetics and spiraling parameters vary across season in a snow dominated mountain stream?
- (3) What are the relative magnitudes of stream physical versus biologic retention of added nitrate across streams from 1st to 4th order?

We addressed these questions by conducting multiple tracer addition experiments in six stream experimental reaches across the stream network and across seasons in one of the stream reaches. We used a combination of traditional and new methods developed in our lab at Montana State University to estimate nitrate retention and uptake dynamics.

References Cited

- Butturini, A. and F. Sabater. 1998. Ammonium and phosphate retention in a Mediterranean stream: hydrological versus temperature control. *Canadian Journal of Fisheries and Aquatic Sciences* **55**:1938-1945.
- Davis, J. C. and G. W. Minshall. 1999. Nitrogen and phosphorus uptake in two Idaho (USA) headwater wilderness streams. *Oecologia* **119**:247-255.
- Dodds, W. K., A. J. Lopez, W. B. Bowden, S. Gregory, N. B. Grimm, S. K. Hamilton, A. E. Hershey, E. Marti, W. H. McDowell, J. L. Meyer, D. Morrall, P. J. Mulholland, B. J. Peterson, J. L. Tank, H. M. Valett, J. R. Webster, and W. Wollheim. 2002. N uptake as a function of concentration in streams. *Journal of the North American Benthological Society* **21**:206-220.
- Galloway, J. N., F. J. Dentener, D. G. Capone, E. W. Boyer, R. W. Howarth, S. P. Seitzinger, G. P. Asner, C. C. Cleveland, P. A. Green, E. A. Holland, D. M. Karl, A. F. Michaels, J. H. Porter, A. R. Townsend, and C. J. Vorosmarty. 2004. Nitrogen cycles: past, present, and future. *Biogeochemistry* **70**:153-226.
- Kaushal, S. S., W. M. Lewis, and J. H. McCutchan. 2006. Land use change and nitrogen enrichment of a Rocky Mountain watershed. *Ecological Applications* **16**:299-312.
- Montana Department of Environmental Quality. 2002. 2002 Montana 303(d) List. http://nris.state.mt.us/wis/environet/2002_303dhome.html.
- Mulholland, P. J., A. M. Helton, G. C. Poole, R. O. Hall, S. K. Hamilton, B. J. Peterson, J. L. Tank, L. R. Ashkenas, L. W. Cooper, C. N. Dahm, W. K. Dodds, S. E. G. Findlay, S. V. Gregory, N. B. Grimm, S. L. Johnson, W. H. McDowell, J. L. Meyer, H. M. Valett, J. R. Webster, C. P. Arango, J. J. Beaulieu, M. J. Bernot, A. J. Burgin, C. L. Crenshaw, L. T. Johnson, B. R. Niederlehner, J. M. O'Brien, J. D. Potter, R. W. Sheibley, D. J. Sobota, and S. M. Thomas. 2008. Stream denitrification across biomes and its response to anthropogenic nitrate loading. *Nature* **452**:202-U246.
- National Science Foundation. 1976. Impacts of large recreational development upon semi-primitive environments, final report. Arlington, VA.
- Newbold, J. D., J. W. Elwood, R. V. Oneill, and W. Vanwinkle. 1981. Measuring nutrient spiralling in streams. *Canadian Journal of Fisheries and Aquatic Sciences* **38**:860-863.

- Peterson, B. J., W. M. Wollheim, P. J. Mulholland, J. R. Webster, J. L. Meyer, J. L. Tank, E. Marti, W. B. Bowden, H. M. Valett, A. E. Hershey, W. H. McDowell, W. K. Dodds, S. K. Hamilton, S. Gregory, and D. D. Morrall. 2001. Control of nitrogen export from watersheds by headwater streams. *Science* **292**:86-90.
- Rabalais, N. N., R. J. Diaz, L. A. Levin, R. E. Turner, D. Gilbert, and J. Zhang. 2010. Dynamics and distribution of natural and human-caused hypoxia. *Biogeosciences* **7**:585-619.
- Stream Solute Workshop. 1990. Concepts and Methods for Assessing Solute Dynamics in Stream Ecosystems. *Journal of the North American Benthological Society* **9**:95-119.
- U.S. Department of Agriculture, F. S. 1994. Ecoregions of the United States: <http://www.fs.fed.us/land/pubs/ecoregions/>.
- Valett, H. M., J. A. Morrice, C. N. Dahm, and M. E. Campana. 1996. Parent lithology, surface-groundwater exchange, and nitrate retention in headwater streams. *Limnology and Oceanography* **41**:333-345.
- Webster, J. R. and B. C. Patten. 1979. Effects of watershed perturbation on stream potassium and calcium dynamics. *Ecological Monographs* **49**:51-72.
- Workshop, S. S. 1990. Concepts and Methods for Assessing Solute Dynamics in Stream Ecosystems. *Journal of the North American Benthological Society* **9**:95-119.

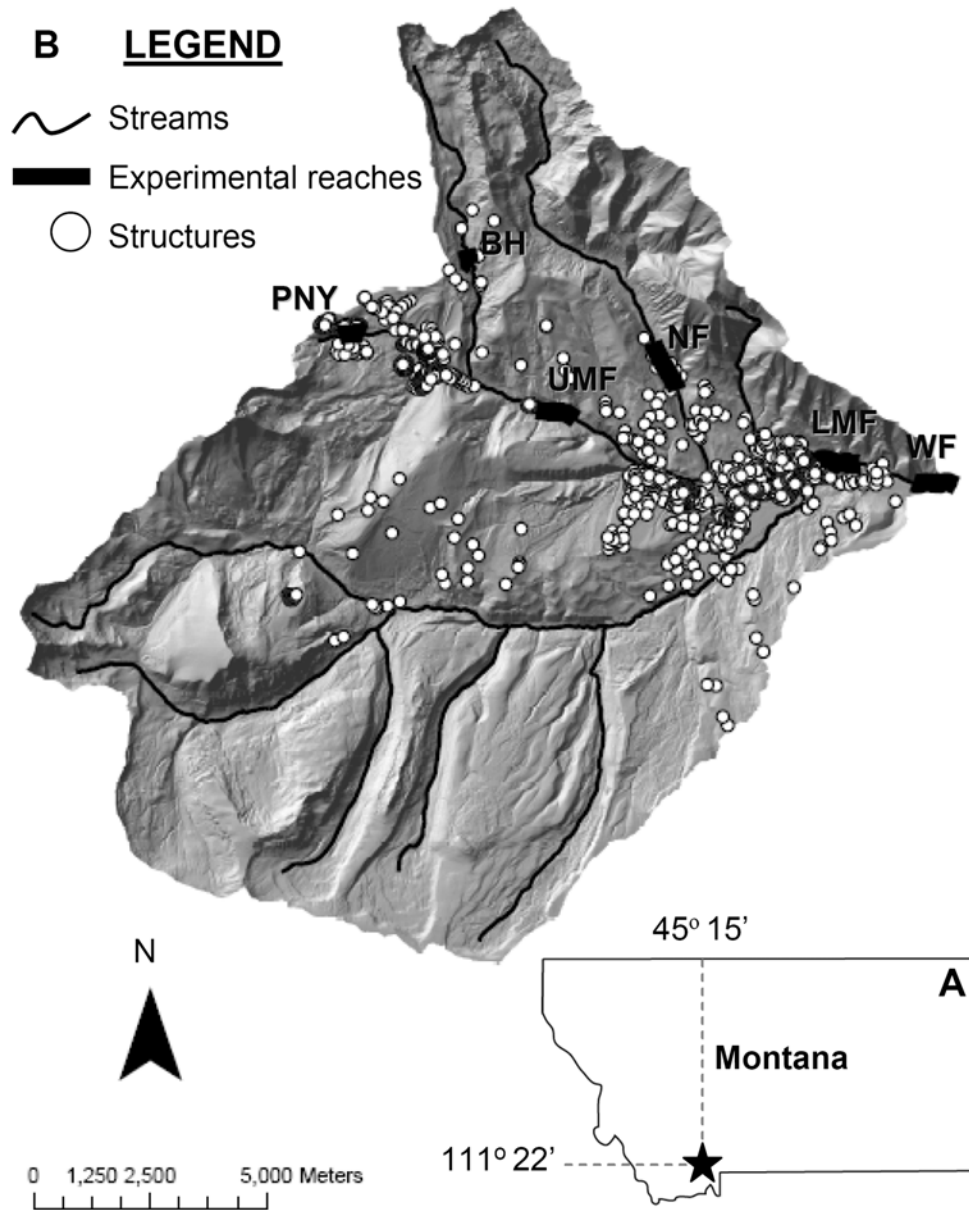


Figure 1.1: (A) Map of Montana showing the location of the West Fork Gallatin Watershed, and (B) shows location of each of the six experimental stream reach within the watershed. The dots on the map represent structure locations. Abbreviated names are next to each experimental stream reach; BH is Beehive, PNY is Pony, UMF is Upper Middle Fork, NF is North Fork, LMF is Lower Middle Fork, and WF is West Fork

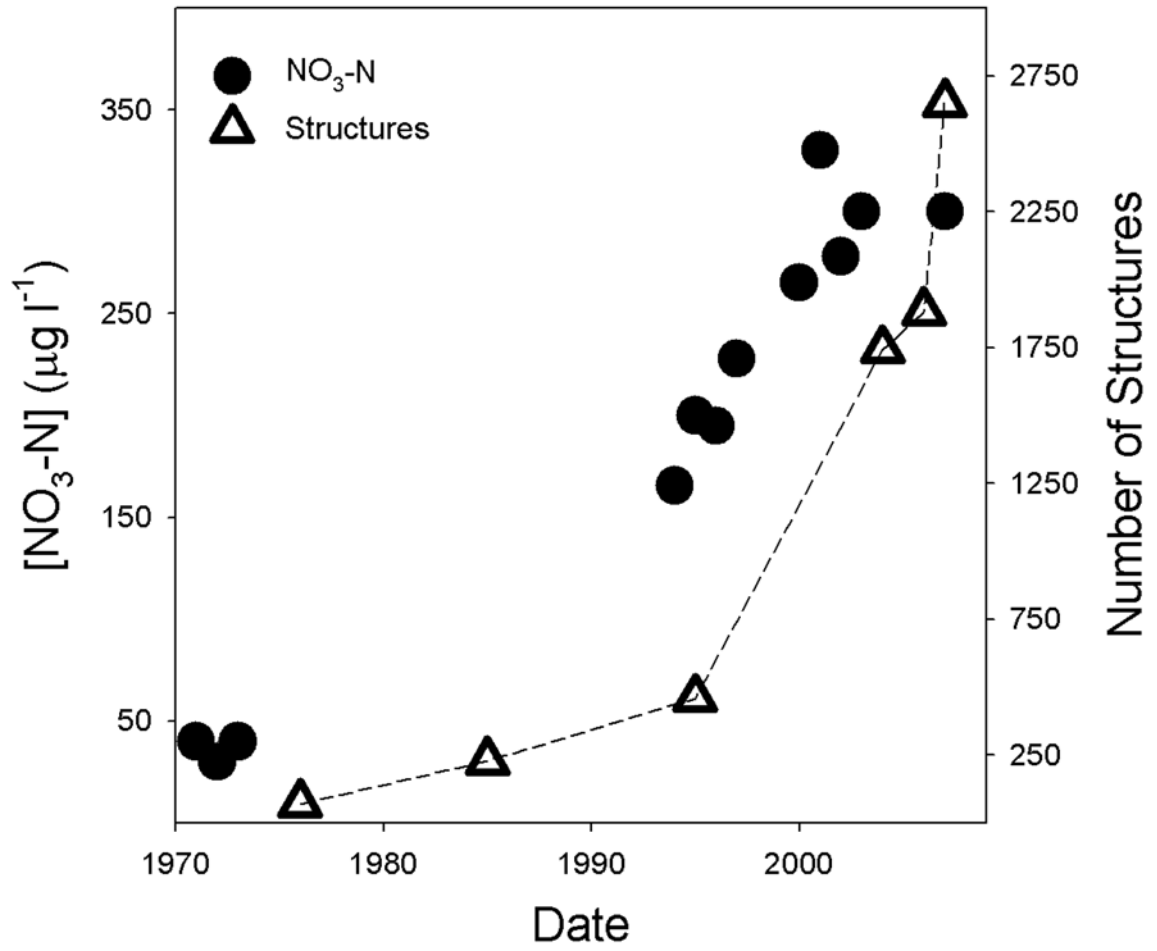


Figure 1.2: Time series of the number of structures and average annual ambient NO₃-N concentrations over the last forty years in the West Fork Gallatin Watershed.

CHAPTER 2

STREAM NITROGEN UPTAKE DYNAMICS FROM
AMBIENT TO SATURATION ACROSS DEVELOPMENT GRADIENTS,
STREAM NETWORK POSITION, AND SEASONSIntroduction

Land use and land cover change is occurring at increasing rates across the Western U.S. Historically, land use in the Western U.S. has been primarily extractive (e.g., mining, logging, ranching, etc.), however, over the last few decades, tourism, recreation, and mountain residences have increased. These shifts in land use and land cover change have increased nutrient loading to many streams (e.g., Whitehead et al. 2002, Biggs et al. 2004, Mueller and Spahr 2006). Nutrients, such as nitrogen (N) and phosphorus (P), are essential to stream biotic activity (Mulholland and Webster 2010). In the Western U.S., however, most headwater streams are oligotrophic with N as the predominant limiting nutrient; therefore excess nutrient can create negative impacts. Nutrient concentrations and/or load in excess (at once or over time) of biotic demand indicates saturation relative to the nutrient of concern (Earl et al. 2006). Excess nutrient is exported downstream, increasing nutrient loading to downstream water bodies (Earl et al. 2006), which can lead to degradation of coastal estuaries and eutrophication of marine environments (Rabalais et al. 2010). Most stream biogeochemistry research has been undertaken in first and second order streams (Ensign and Doyle 2006), however the effects of stream nutrient retention and uptake dynamics in headwater streams on downstream export are not well understood (but see Peterson et al. 2001).

The concept of stream nutrient spiraling was introduced in the late 1970s and early 1980s (Webster and Patten 1979, Newbold et al. 1981); it was quickly understood that shorter spiraling lengths indicated more efficient nutrient cycling in the systems (Newbold et al. 1981). About a decade after the concept of nutrient spiraling was introduced, the Stream Solute Workshop (1990) formalized much of the nutrient spiraling theory and methodological approaches that subsequent experiments have followed (i.e., constant-rate/plateau approach) (e.g., Hart et al. 1992, Davis and Minshall 1999, Dodds et al. 2002, Hall et al. 2002, Mulholland et al. 2002, Webster and Valett 2006).

Some studies have demonstrated that nutrient uptake can vary substantially among seasons within the same stream reach (Mulholland et al. 1985, Marti and Sabater 1996, Simon et al. 2005) and that seasonality can cause larger variation in nitrate retention than stream-size (Alexander et al. 2009). In areas of rapid development, such as in the West Fork Gallatin Watershed, Big Sky, Montana anthropogenic nutrient loading can be large (Gardner and McGlynn 2009). Even modest additions of nutrients can increase concentrations downstream; increases in concentration caused by additions vary across seasons (Kaushal et al. 2006). Nitrate loading can vary temporally due to both natural and anthropogenic inputs (Kennedy et al. 2009). With increased loading there can also be a decrease in uptake efficiency (Earl et al. 2006). Additionally, Butturini and Sabater (1998) found that temperature played an important role in nutrient retention when discharge was low. The variability of nutrient retention associated with temperature changes (i.e., seasonality) is likely due to changes in biotic activity (Marti and Sabater 1996). Therefore, high $\text{NO}_3\text{-N}$ concentrations during periods of low biological uptake

potential (seasonally or diurnally), could lead to increases in the amount of $\text{NO}_3\text{-N}$ exported downstream.

In-stream nutrient processing can also vary with stream characteristics which vary across watersheds. As stream size increases so does velocity (Wondzell et al. 2007), which can decrease nutrient retention and uptake (Valett et al. 1996, Butturini and Sabater 1998). To date, most nutrient retention and uptake dynamic studies have been conducted on a single-reach scale (e.g., Dodds et al. 2002, Ensign and Doyle 2006, O'Brien et al. 2007, Mulholland et al. 2008, Hall et al. 2009) primarily in first and second order streams (Ensign and Doyle 2006). Some studies have been conducted on multiple reaches along the same stream network (Covino et al. 2010) or on multiple single-reaches within watersheds in close proximity (Royer et al. 2004). Most research focused on network scale nutrient export dynamics has been model-based (Alexander et al. 2009, Claessens and Tague 2009).

Land use and land cover changes can increase nutrient loading to headwater streams (Kaushal et al. 2006) and these increased loads can affect stream network's ability to retain nutrients from the water column (Earl et al. 2006). Thousands of tracer experiments have been conducted world wide at the single-reach stream scale, yet it is not well understood how nutrient retention and uptake vary at the watershed or stream network scale, how the effects differ within watersheds that have varying development intensities, or how seasonality affects retention in mountain environments. Nitrogen levels in the West Fork Gallatin Watershed have increased due to increased development and septic inputs (RANN study by the National Science Foundation (National Science

Foundation 1976), see also Blue Water Task Force, unpublished data, 2000–2005 and Big Sky Water and Sewer District, unpublished data, 1994–1999, (Gardner and McGlynn 2009)). Streams can play an important role in buffering biogeochemical processes following anthropogenic disturbances (Bernhardt et al. 2003). One component to understanding and predicting the fate and transport of N in environments like the West Fork Gallatin Watershed is investigating and quantifying how N is assimilated or cycled through in-stream and stream network processes. Both biological (i.e., uptake) and physical (i.e., hydrological) processes drive nutrient retention from the water column. Physical retention (e.g., in the hyporheic zone) can increase the potential for later biological uptake (Triska et al. 1989a, b). Mass recovery calculation is an important component in understanding the water balance of gains and losses between streams and groundwater along a stream reach and how this influences physical nutrient retention (Payn et al. 2009); additionally stream water gains and losses can also affect ambient stream water chemistry (Covino and McGlynn 2007).

Application of traditional stream spiraling experimental approaches (i.e., constant-rate/plateau approach outlined in the Stream Solute Workshop (1990)) has demonstrated increased uptake lengths for both N and P with increased nutrient concentration (Hart et al. 1992, Dodds et al. 2002, Mulholland et al. 2002). Therefore, nutrient addition experiments can lead to overestimated ambient uptake lengths (Mulholland et al. 2002). We seek to build on retention and uptake dynamics learned through conducting traditional tracer addition experiments by quantifying uptake as a function of concentration. Recently, we have developed less cost and time-prohibitive

methods (Covino et al. 2010, Covino et al. in press) that turn previously believed limitations of nutrient addition experiments into strengths. Using the recently developed Tracer Additions for Spiraling Curve Characterization (TASCC) method (Covino et al. 2010, Covino et al. in press), one can characterize stream nutrient uptake dynamics from ambient to saturation with one instantaneous nutrient addition experiment. These spiraling concentration curves can be used to assign appropriate kinetic models that reflect stream uptake response across a range of concentrations. Total reach scale retention of added $\text{NO}_3\text{-N}$ (including biological and physical) can also be calculated using methods outlined by Covino et al. (2010). We conducted multiple tracer addition experiments to obtain a better understanding of nitrate retention and uptake dynamics across the West Fork Gallatin Watershed and we address the following specific questions:

- (1) How do stream uptake kinetics and spiraling parameters vary across streams of different development intensity and scale?
- (2) How do uptake kinetics and spiraling parameters vary across season in a snow dominated mountain stream?
- (3) What are the relative magnitudes of stream physical versus biologic retention of added nitrate across streams from 1st to 4th order?

Methods

Study Area

This research was conducted in the Northern Rocky Mountains in the Madison Mountain Range of Southwestern Montana, USA. Multiple tracer addition experiments were conducted at six sites throughout the West Fork Gallatin Watershed. The six streams had varying watershed area (WA), stream discharge (Q), stream order, number of structures (including residential and commercial), ambient $\text{NO}_3\text{-N}$ concentrations [$\text{NO}_3\text{-}N_{amb}$], and average annual $\text{NO}_3\text{-N}$ concentrations (Tables 1 and 2 and Figure 2.1).

The three main subwatersheds in the West Fork Gallatin Watershed (240 km^2) are the South Fork Gallatin (121 km^2), the Middle Fork Gallatin (48 km^2), and the North Fork Gallatin (24 km^2) with the primary streams flowing from west to east. The elevation ranges from 1800 to 3400 m with well-defined steep topography and shallow soils. Dominant geology in the West Fork Watershed is varied. In the valley bottoms, surficial geology is largely colluvium and glacial deposits while higher elevations are mainly comprised of sedimentary (e.g. gravel deposits) and metasedimentary (e.g. granitic gneiss) formations of various ages and metamorphosed volcanics of Archean age. From low to high elevations, precipitation ranges from less than 50 cm to more than 127 cm annually with the majority of precipitation falling as snow during the winter and spring months (Lone Mountain NRCS SNOTEL #590, 2707 m elevation). The growing season is short with 75-90 frost free days (fewer frost free days with increased elevation) from mid-June to mid-September (U.S. Department of Agriculture 1994). In the higher elevations of the watershed, vegetation predominantly is coniferous forest (Lodgepole

pine (*Pinus contorta*), Blue spruce (*Picea pungens*), Engelmann spruce (*Picea engelmannii*) and Douglas fir (*Pseudotsuga menziesii*) and native grasses with willows (*Salix spp.*) and aspen (*Populus tremuloides*) groves in the riparian areas. Vegetation in the lower elevations is similar but is dominated by native grasses, shrubs and willows (*Salix spp.*) with fewer coniferous trees.

Seventeen stream tracer addition experiments were conducted throughout the watershed in six stream reaches (Figure 2.1). Nitrogen uptake and spiraling metric dynamics were determined from data collected during the tracer addition experiments. In the Middle Fork Gallatin Watershed, experiments were conducted in four stream reaches: Beehive, Pony, Upper Middle Fork, and Lower Middle Fork. One experimental location was located in the North Fork Gallatin Watershed: North Fork. The final stream reach, West Fork, extended from the West Fork Gallatin's confluence with the Gallatin River to approximately 1100 meters upstream of the confluence (Figure 2.1). Please see tables 1 and 2 for additional information on the six stream reaches, their corresponding characteristics, and the season in which experiments occurred.

Experimental Design

Multiple experiments were conducted across six stream reaches throughout the West Fork Gallatin Watershed to determine how stream NO₃-N uptake and retention dynamics vary with respect to development intensity, watershed area, and season (Figure 2.1). Land use and land cover change in the West Fork Watershed is primarily due to human development, both residential and commercial. Increased development and increased numbers of structures are positively correlated with an increase in ambient

stream water $\text{NO}_3\text{-N}$ concentrations (Figures 2.1 and 2.2). We paired four of the six streams in our analysis based on varying watershed area (WA), stream discharge (Q), and ambient $\text{NO}_3\text{-N}$ concentrations [$\text{NO}_3\text{-N}_{amb}$]. The stream reaches were paired for comparison of uptake kinetics and spiraling parameters between high and low instream [$\text{NO}_3\text{-N}_{amb}$] for streams of similar scale (both watershed area and discharge). Pony and Beehive were paired as the two small stream reaches (WA and Q), Pony had high [$\text{NO}_3\text{-N}_{amb}$] and Beehive had low [$\text{NO}_3\text{-N}_{amb}$] (Table 1, Figure 2.1). North Fork and Upper Middle Fork were paired as the two medium sized streams (WA and Q), North Fork had low [$\text{NO}_3\text{-N}_{amb}$] and Upper Middle Fork had high [$\text{NO}_3\text{-N}_{amb}$] (Table 1, Figure 2.1). Lower Middle Fork and West Fork were not paired as Lower Middle Fork is the upstream part of the main stem of the West Fork. West Fork is the experimental reach ending at the confluence with the Gallatin River. Across the six stream reaches, discharge (Q) during the experiments varied by three orders of magnitude and [$\text{NO}_3\text{-N}_{amb}$] varied by one order of magnitude (Table 2). Four additional experiments were conducted in the Beehive experimental reach to explore seasonal changes in $\text{NO}_3\text{-N}$ uptake and retention dynamics. Discharge (Q) during the seasonal experiments ranged over two orders of magnitude and [$\text{NO}_3\text{-N}_{amb}$] varied by nearly two orders of magnitude (Table 2). For additional background water quality and watershed information please see Gardner and McGlynn (2009). The stream tracer addition experiments were conducted in the summer (July and August) of 2007 and 2008 with the exception of Beehive where a series of five seasonal experiments were performed.

Stream Discharge

Prior to conducting tracer addition experiments, stream discharge was measured at downstream (base) and upstream (head) endpoints of each experimental reach using dilution gauging methods. A pre-weighed amount of NaCl (a conservative tracer) was fully dissolved in a 20 liter bucket of stream water then added as an instantaneous addition to the stream at a predetermined location (20 – 100 meters upstream of the downstream measurement location). Specific conductance (SC) was measured in real-time at two second intervals at the downstream measurement location with Campbell Scientific (Logan, UT) CS547A temperature and conductivity probes connected to Campbell Scientific CR1000 data loggers. We quantified the relationship between SC and NaCl concentration ($r^2 = 0.999$, $p < 0.0001$) and from this relationship and breakthrough curve (BTC) integration, we calculated stream Q (Day 1976, Kilpatrick and Cobb 1985, Dingman 2002). The tracer BTC is defined as the change in tracer concentration over time and is measured at a location downstream.

Stream Tracer Experiments using Constant-rate Additions of Cl and NO₃-N

Field Methods and Chemical Analysis: Constant-rate additions were conducted on two of the six reaches (Beehive and Lower Middle Fork). Stream reaches varied in length from 588 – 1286 meters, respectively, between the two streams. The stream reaches had 10 – 12 longitudinal sampling sites evenly spaced along each reach, including a sampling site at both the downstream and upstream endpoints; the upstream endpoint was above potential tracer influence. Modified methods from Webster and

Valett (2006) were used to conduct the constant-rate tracer addition experiments. Dependant on stream $[NO_3-N_{amb}]$ and Q , we added a solution of fully dissolved NaCl (conservative tracer) and KNO_3 (biologically-active tracer) from a carboy of known volume to the stream at a constant-rate using a Fluid Metering pump (Fluid Metering Inc., Syosset, NY). Specific conductance (SC) and temperature were measured real-time as described previously. SC and temperature data were collected at both the downstream and upstream endpoints of each stream reach at ten second intervals through the experimental period starting before any tracer additions until after the last sample was collected. Stream nutrient spiraling was calculated from the longitudinal decline in NO_3-N concentration relative to the Cl concentration during the plateau portion of a constant rate injection. Once the stream reached SC plateau based on observed SC at the downstream endpoint, longitudinal samples were collected moving upstream from the downstream endpoint. Stream water samples were also collected on 30 second to 10 minute intervals during the rising and falling limbs to and from plateau concentrations. Frequency of sampling depended on the slope of the rising and falling limbs; samples were taken more frequently during times of greater rates of change in concentration.

Samples were either filtered on site and kept in a cooler at $\sim 4^\circ C$ or kept in a cooler and filtered at the lab within 24 hours using Isopore Polycarbonate Membrane filters with a $0.4 \mu m$ pore size (Millipore, Billerica, MA). Filtered samples were frozen in high-density polyethylene bottles until analysis. Each sample was analyzed for chloride (Cl^-) and nitrate (NO_3^-) by ion-exchange chromatography using a Metrohm IC equipped with a 150×4.0 mm column (Metrohm Corp., Herisau, Switzerland). A $200 \mu l$

injection volume was used for low-level detection of anions. The analytical detection limits for NO_3^- and Cl^- were 5 and 2 $\mu\text{g l}^{-1}$, respectively. Standards prepared from reagent-grade salts were routinely checked against certified Alltech brand standards during every IC run. Field and lab replicates were also included in every IC run.

Calculating $\text{NO}_3\text{-N}$ Spiraling Parameters using the Plateau Approach: All stream $\text{NO}_3\text{-N}$ uptake dynamics quantification followed the methods detailed in Covino et al. (in press; Covino et al. 2010). Longitudinal stream samples collected during the plateau portion of the constant-rate additions were used to calculate uptake length (S_w) (Stream Solute Workshop 1990). The slope of the linear regression between the natural log of $\text{NO}_3\text{-N}:\text{Cl}$ of the longitudinal stream samples and the distance downstream from the injection site yielded a longitudinal uptake rate of plateau approach added nutrient ($k_{w\text{-add-plat}}$). The plateau approach uptake length of added nutrient is the negative inverse of $k_{w\text{-add-plat}}$ ($S_{w\text{-add-plat}}$) (Eq. 1).

$$\text{Eq. 1 } S_{w\text{-add-plat}} = -1/k_{w\text{-add-plat}}$$

Areal uptake rate of added nutrient for the plateau approach ($U_{\text{add-plat}}$) was calculated from $S_{w\text{-add-plat}}$ and added nutrient uptake velocity ($V_{f\text{-add-plat}}$) was calculated from $U_{\text{add-plat}}$ (Eqs. 2 and 3):

$$\text{Eq. 2 } U_{\text{add-plat}} = (Q \times [\text{NO}_3^- \text{N}_{\text{add-plat}}]) / (w \times S_{w\text{-add-plat}})$$

$$\text{Eq. 3 } V_{f\text{-add-plat}} = U_{\text{add-plat}} / [\text{NO}_3^- \text{N}_{\text{add-plat}}]$$

where Q is the stream discharge ($L^3 T^{-1}$), $[NO_3-N_{add-plateau}]$ is the geometric mean of background corrected NO_3-N concentrations of the longitudinal stream samples collected during plateau ($M L^{-3}$), and w is average wetted stream width (L).

Stream Tracer Experiments using Instantaneous Slug Additions of Cl and NO_3-N

Field Methods and Chemical Analysis: The six stream reaches varied in length from 523 – 1286 meters depending on stream size (i.e., streams with higher discharge had longer reach lengths) (Table 2). We instantaneously added (i.e., slug addition) a solution of dissolved NaCl (conservative tracer) and KNO_3 (biologically-active tracer) at the upstream endpoint of each stream reach. The masses of NaCl and KNO_3 added were dependant on stream $[NO_3-N_{amb}]$ and Q . Specific conductance (SC) and temperature were measured real-time using the equipment described previously. SC and temperature data were collected at both the downstream and upstream endpoints of each stream reach at ten second intervals through the experimental period starting before any additions and continuing until after the last sample was collected (i.e., return to background conditions with no influence of added tracers). Stream water samples were collected on 30 second to 10 minute intervals depending on the slope of the breakthrough curve (BTC); samples were taken more frequently during periods of greater concentration change over the BTC. For our experiments, the BTC was measured at the base of the reach (i.e., 523 – 1286 m downstream) for each stream reach (Figure 2.4 A). Stream water samples were filtered, handled, and analyzed identically to the ones collected during constant-rate additions.

Mass Recovery of Cl and NO₃-N: We used an approach similar to Ruggiero et al. (2006) and Tank et al. (2008) to determine the mass of tracer recovered (Cl and NO₃-N in our experiments) from the initial mass of injected tracer. Mass recovered is the product of the time-integrated tracer concentrations from every sample and Q at the downstream endpoint (base) for each stream reach (Eq. 4):

$$\text{Eq. 4} \quad T_{MR} = Q \times \int_0^t T_C(t) dt$$

where T_{MR} is the mass of tracer (Cl or NO₃-N) recovered and T_C is the time-integrated tracer (Cl or NO₃-N) concentration (M T L⁻³). We calculated mass loss from T_{MR} (Eq. 5):

$$\text{Eq. 5} \quad \text{Mass Loss} = \text{Mass Injected} - T_{MR}$$

where *Mass Loss* is the mass of tracer not recovered from the *Mass Injected* and *Mass Injected* is the mass of tracer added to the stream at the upstream endpoint. Because NO₃-N mass loss can be attributed to both biological and physical processes, we defined three categories of NO₃-N retention: physical retention (*PR*), biological retention (*BR*), which added together represent total retention (*TR*). In Eq. 6, *TR* is analogous to *Mass Loss* from equation Eq. 5.

$$\text{Eq. 6} \quad TR = \text{Mass of NO}_3^- \text{N added} - T_{MR} \text{ - NO}_3^- \text{N}$$

Where *TR* is the amount of NO₃-N added at the upstream endpoint that is not measured at the downstream endpoint, *Mass of NO₃-N added* is the total NO₃-N mass injected at the upstream endpoint and $T_{MR}\text{-NO}_3\text{-N}$ is the mass of NO₃-N recovered at the downstream endpoint. We assume percent physical retention of NO₃-N to be equal to Cl % retention. Using Eq. 7, we calculated physical retention (*PR*) of NO₃-N:

$$\text{Eq. 7 } PR = (100 - T_{MR} - Cl(\%)) \times \text{Mass of } NO_3\text{-N added}$$

where $T_{MR} - Cl(\%)$ is the percent of Cl added at the upstream endpoint that was recovered at the downstream endpoint. Biological retention (BR) of $NO_3\text{-N}$ during the experiment was the difference between total retention (TR) and physical retention (PR) (Eq. 8).

$$\text{Eq. 8 } BR = TR - PR$$

Because percent physical retention of $NO_3\text{-N}$ is assumed to be equal to the percent Cl retention, the difference between TR and PR is assumed to be BR during the BTC for the instantaneous tracer addition. Also, PR is only defined for the timescale of the experiment, a portion of the $NO_3\text{-N}$ that was physically retained could eventually return to the stream and some of the physically retained $NO_3\text{-N}$ could ultimately be biologically retained.

Calculating Breakthrough Curve-integrated Stream $NO_3\text{-N}$ Concentration: As the instantaneous tracer addition solutes travel downstream, $NO_3\text{-N}$ added to the stream is retained from the water column partially as a function of stream $NO_3\text{-N}$ concentration. To determine a BTC-integrated $NO_3\text{-N}$ concentration, for reference we calculated the geometric mean of the observed and conservative $NO_3\text{-N}$ concentrations. Conservative $NO_3\text{-N}$ was defined as the $NO_3\text{-N}$ concentration that would have been observed had it travelled conservatively (based on observed Cl and the injectate ratio, which represents the maximum amount of $NO_3\text{-N}$ that could arrive at the base of the experimental reach) integrated over the BTC ($M L^{-3}$) (Eq. 9):

$$\text{Eq. 9 } [NO_3-N_{add-int}] = \sqrt{\frac{\int_0^t [NO_3-N_{add-obs}](t)dt}{\int_0^t Q(t)dt} \times \frac{\int_0^t [NO_3-N_{cons}](t)dt}{\int_0^t Q(t)dt}}$$

where $[NO_3-N_{add-int}]$ is the geometric mean of background corrected observed and conservative NO_3-N concentrations integrated over the BTC, $[NO_3-N_{add-obs}]$ is the observed NO_3-N concentration ($M L^{-3}$) in the grab sample collected throughout the BTC (this concentration is background corrected), and $[NO_3-N_{cons}]$ is the NO_3-N concentration ($M L^{-3}$) that one would expect to measure throughout the BTC in each grab sample if NO_3-N traveled through the system conservatively (i.e., the maximum concentration that could be observed).

Calculating Stream NO_3-N Uptake Dynamics through BTC-integration: We used an approach similar to Tank et al. (2008) to determine BTC-integrated uptake lengths of added nutrient ($S_{w-add-int}$) for each instantaneous tracer addition. With Eq. 4, we determined T_{MR} for both Cl and NO_3-N for each of the samples taken during the BTC of an instantaneous tracer addition. We calculated the BTC-integrated uptake length of added nutrient ($S_{w-add-int}$) from the T_{MR} . The slope between the natural log of $NO_3-N:Cl$ of the injectate and the natural log of the ratio of T_{MR-NO_3-N} to T_{MR-Cl} across the BTC against stream reach distance yielded the added nutrient BTC-integrated longitudinal uptake rate ($k_{w-add-int}$) (Figure 2.3 B). The negative inverse of $k_{w-add-int}$ is the added nutrient BTC-integrated uptake length ($S_{w-add-int}$) for the instantaneous addition (Eq. 10).

$$\text{Eq. 10 } S_{w-add-int} = -1/k_{w-add-int}$$

From $S_{w-add-int}$, we calculated BTC-integrated added nutrient areal uptake rates ($U_{add-int}$) (Figure 2.3 D) and uptake velocities ($V_{f-add-int}$) (Eqs. 11 and 12).

$$\text{Eq. 11 } U_{add-int} = (Q \times [NO_3^- N_{add-int}]) / (w \times S_{w-add-int})$$

$$\text{Eq. 12 } V_{f-add-int} = U_{add-int} / [NO_3^- N_{add-int}]$$

Calculating Stream NO₃-N Uptake Dynamics using the TASCC Method: We calculated dynamic uptake length ($S_{w-add-dyn}$) for each sample across the BTC using a recently developed technique (Covino et al. 2010, Covino et al. in press), the Tracer Additions for Spiraling Curve Characterization (TASCC) method. The slope of the line fit to the natural log of NO₃-N:Cl ratios of the injectate and each grab sample collected across the BTC against stream distance equals the dynamic added nutrient uptake rate ($k_{w-add-dyn}$) (Figure 2.3 B). To calculate a dynamic added nutrient uptake length ($S_{w-add-dyn}$) for each sample from the BTC, we calculated the negative inverse of each $k_{w-add-dyn}$ (Eq. 13).

$$\text{Eq. 13 } S_{w-add-dyn} = -1 / k_{w-add-dyn}$$

From $S_{w-add-dyn}$ we calculated dynamic areal uptake rates of added nutrient ($U_{add-dyn}$) (Figure 2.3 D) and dynamic uptake velocities of added nutrient ($V_{f-add-dyn}$) (Eqs. 14 and 15):

$$\text{Eq. 14 } U_{add-dyn} = (Q \times [NO_3^- N_{add-dyn}]) / (w \times S_{w-add-dyn})$$

$$\text{Eq. 15 } V_{f-add-dyn} = U_{add-dyn} / [NO_3^- N_{add-dyn}]$$

where $[NO_3^- N_{add-dyn}]$ is geometric mean of observed (background corrected) and conservative NO₃-N concentration (M L⁻³) of the single grab sample.

Ambient and Total NO₃-N Uptake
Dynamics and Kinetic Model Parameters

Calculating Ambient Stream NO₃-N Uptake Parameters: We calculated ambient uptake length (S_{w-amb}) for each stream reach using each of the previously calculated $S_{w-add-dyn}$ values and the method developed by Payn et al. (2005). To determine S_{w-amb} , we calculated the y-intercept from the linear regression of NO₃-N_{tot-dyn} versus $S_{w-add-dyn}$ (Figure 2.3 C). Ambient areal uptake rate (U_{amb}) was calculated from S_{w-amb} (Eq. 16):

$$\text{Eq. 16 } U_{amb} = (Q \times [NO_3 - N_{amb}]) / (w \times S_{w-amb})$$

and the ambient uptake velocity (V_{f-amb}) was calculated from U_{amb} (Eq. 17):

$$\text{Eq. 17 } V_{f-amb} = U_{amb} / [NO_3 - N_{amb}]$$

where $[NO_3 - N_{amb}]$ is the ambient stream NO₃-N concentration (M L⁻³).

Calculating Total Stream NO₃-N Concentrations Associated with Tracer Addition

Experiments: For the plateau approach, the total NO₃-N concentration $[NO_3 - N_{tot-plat}]$ is the geometric mean of total NO₃-N concentrations (non-background corrected) (M L⁻³) for all (10 – 12 samples depending on the stream reach) of the longitudinal stream samples collected during the plateau of the constant-rate addition. We used different total NO₃-N concentrations for each method of calculating uptake parameters from an instantaneous addition: $NO_3 - N_{tot-int}$ for the BTC-integrated approach and $NO_3 - N_{tot-dyn}$ for the dynamic TASC approach. The two NO₃-N concentrations for the instantaneous addition method were calculated using Eqs. 18 and 19:

$$\text{Eq. 18 } [NO_3-N_{tot-int}] = \sqrt{\frac{\int_0^t Q [NO_3-N_{tot-obs}](t) dt}{\int_0^t Q(t) dt} \times \frac{\int_0^t Q [NO_3-N_{cons}] + [NO_3-N_{amb}](t) dt}{\int_0^t Q(t) dt}}$$

$$\text{Eq. 19 } [NO_3-N_{tot-dyn}] = \sqrt{[NO_3-N_{tot-obs}] \times ([NO_3-N_{cons}] + [NO_3-N_{amb}])}$$

where $[NO_3-N_{tot-int}]$ is the geometric mean of non-background corrected total observed and conservative NO_3-N BTC-integrated concentrations ($M L^{-3}$), $[NO_3-N_{tot-obs}]$ is the total observed NO_3-N concentration ($M L^{-3}$) in the samples collected throughout the BTC (note that this concentration is not background corrected), $[NO_3-N_{cons}]$ is the NO_3-N concentration ($M L^{-3}$) that we would expect to measure throughout the BTC in each sample if NO_3-N traveled through the system conservatively (i.e., the maximum concentration that could be observed), and $[NO_3-N_{tot-dyn}]$ is the geometric mean of the total observed (non-background corrected) and conservative NO_3-N concentration ($M L^{-3}$) associated with each grab sample.

Calculating Stream Total NO_3-N Uptake Parameters: We calculated total uptake parameters for each stream reach. Total areal uptake ($U_{tot-plat}$, $U_{tot-int}$, and $U_{tot-dyn}$) was calculated as the sum of ambient and added nutrient spiraling values (Eqs. 20, 21, and 22):

$$\text{Eq. 20 } U_{tot-plat} = U_{amb} + U_{add-plat}$$

$$\text{Eq. 21 } U_{tot-int} = U_{amb} + U_{add-int}$$

$$\text{Eq. 22 } U_{tot-dyn} = U_{amb} + U_{add-dyn}$$

where $U_{tot-plat}$ is the total areal uptake rate ($M L^{-2} T^{-1}$) from the plateau approach, $U_{tot-int}$ is the total areal uptake rate from the BTC-integrated ($M L^{-2} T^{-1}$), and $U_{tot-dyn}$ is the total dynamic areal uptake rate ($M L^{-2} T^{-1}$) for each grab sample (Figure 2.3 D). Total dynamic uptake velocity was calculated using Eqs. 23, 24, and 25:

$$\text{Eq. 23 } V_{f-tot-plat} = U_{tot-plat} / [NO_3^- - N_{tot-plat}]$$

$$\text{Eq. 24 } V_{f-tot-int} = U_{tot-int} / [NO_3^- - N_{tot-int}]$$

$$\text{Eq. 25 } V_{f-tot-dyn} = U_{tot-dyn} / [NO_3^- - N_{tot-dyn}]$$

where $V_{f-tot-plat}$ is the total uptake velocity from the plateau approach ($L T^{-1}$), $V_{f-tot-int}$ is the total uptake velocity ($L T^{-1}$) from the BTC-integrated, and $V_{f-tot-dyn}$ is the total dynamic uptake velocity ($L T^{-1}$) for each grab sample from the BTC.

Calculating Maximum Areal Uptake Rate and Half-Saturation Constant using the Michaelis-Menten Kinetic Model: We used an M-M hyperbolic relationship between $[NO_3^- - N_{tot-dyn}]$ and $U_{tot-dyn}$ to determine a maximum areal uptake rate (U_{max}) and a half-saturation constant (K_m) for each stream reach (Earl et al. 2006, Newbold et al. 2006) (Eq. 26):

$$\text{Eq. 26 } U_{tot-dyn} = (U_{max} \times [NO_3^- - N_{tot-dyn}]) / ([NO_3^- - N_{tot-dyn}] + K_m)$$

where U_{max} is the maximum areal uptake rate ($M L^{-2} T^{-1}$). Please see Covino et al. (in press) for a more detailed description of the methods outlined in this article.

Results

Variability in Measured Stream Discharge across Experimental Reaches

Tracer addition experiments were performed after peak snowmelt runoff, during summer baseflow discharge conditions. Stream discharge (Q) values across the six stream reaches varied by three orders of magnitude. The lowest Q was measured in Pony ($0.006 \text{ m}^3 \text{ s}^{-1}$) and the greatest in West Fork ($2.47 \text{ m}^3 \text{ s}^{-1}$) (Table 2).

Physical and Biological Retention of Added $\text{NO}_3\text{-N}$

Total, physical, and biological retention of added $\text{NO}_3\text{-N}$ was determined using a mass balance approach. Physical and biological retention of added $\text{NO}_3\text{-N}$ varied relative to watershed size (Figure 2.4 A, B and Tables 2 and 3). For the six experimental reaches, watershed areas range from $< 1 \text{ km}^2$ at the downstream endpoint of the Pony experimental reach to $> 200 \text{ km}^2$ at the downstream endpoint of the West Fork stream reach. An increase in watershed area generally led to a decrease in physical retention and an increase in biological retention of added $\text{NO}_3\text{-N}$ (Figure 2.4 A, B and Tables 2 and 3). Across the six sites, physical retention ranged from 8 to 81% of added $\text{NO}_3\text{-N}$ and biological retention ranged from 5.5 to 57% of added $\text{NO}_3\text{-N}$. The greatest physical retention of added $\text{NO}_3\text{-N}$ (81%) occurred in the smallest watershed/stream (Pony) and the greatest biological retention of added $\text{NO}_3\text{-N}$ (57%) was measured in the largest watershed/stream (West Fork). The relationship between the ratios of biological to total retention of added $\text{NO}_3\text{-N}$ versus watershed area was similar to biological retention of

added $\text{NO}_3\text{-N}$ versus watershed area. An increase in watershed area led to an increased ratio of biological to total retention of added $\text{NO}_3\text{-N}$, meaning as watershed area increased biological retention comprised a larger portion of total retention of added $\text{NO}_3\text{-N}$ (Figure 2.4 C). We observed an inverse relationship between biological and physical retention of added $\text{NO}_3\text{-N}$. Physical retention was greatest in small stream reaches with low biological retention, and *vice versa* (Figure 2.4 D). In the West Fork experimental reach located at the mouth of the 240 km^2 watershed, 65.3 and 64.6% of the $\text{NO}_3\text{-N}$ added during two consecutive (i.e., conducted on the same day, the second slug was injected after specific conductance returned to background levels at the base of the experimental reach) instantaneous tracer addition experiments (27.7 and 277 g added $\text{NO}_3\text{-N}$) was retained. Peak nutrient concentrations of 9.62 and 111 $\mu\text{g l}^{-1}$ above background were reached and ~35% of the added $\text{NO}_3\text{-N}$ from each of the two additions was exported into the Gallatin River (a tributary to the Missouri River) and ~65% was retained over the time scale of the experiment.

Ambient Uptake Dynamics

Ambient uptake lengths ($S_{w\text{-}amb}$) varied from 624 – 1265 m across the West Fork Gallatin Watershed (Table 4 and Figure 2.5). For five of the six stream reaches (excluding West Fork), increased $[\text{NO}_3\text{-N}_{amb}]$ had a strong correlation with decreased $S_{w\text{-}amb}$ ($r^2 = 0.95$, p-value = 0.005, with West Fork $r^2 = 0.35$, p-value = 0.22) (Figure 2.5). Increased average annual $\text{NO}_3\text{-N}$ concentrations had a strong correlation to decreased $S_{w\text{-}amb}$ for all six reaches, ($r^2 = 0.72$, p-value = 0.03) (Figure 2.5). For each of the pairs (Beehive-Pony and North-Fork: Upper Middle Fork), the stream with a higher ambient

$\text{NO}_3\text{-N}$ had the shorter $S_{w\text{-}amb}$. The two streams with higher ambient $\text{NO}_3\text{-N}$ (Pony and Upper Middle Fork) had $S_{w\text{-}amb}$ values of 625 m and 1020 m, respectively (Table 4). The two streams with lower $[\text{NO}_3\text{-N}_{amb}]$ (Beehive and North Fork) had longer $S_{w\text{-}amb}$ values (1171 m and 1265 m) (Table 4). The West Fork (the largest stream) had an $S_{w\text{-}amb}$ nearly identical to the smallest stream (Pony) (624 m and 625, respectively) despite West Fork having the second lowest $[\text{NO}_3\text{-N}_{amb}]$ and Pony the highest $[\text{NO}_3\text{-N}_{amb}]$ (3.96 and 68.31 $\mu\text{g l}^{-1}$, respectively) (Table 4 and Figure 2.5).

There was a significant relationship between increased watershed area and increased ambient areal uptake rate (U_{amb}) (p-value = 0.03, Figure 2.6 A). Watershed area ranged from 0.9 to 240 km^2 (from Pony to West Fork, respectively) with a range in U_{amb} from 9.99 to 232 ($\mu\text{g m}^{-2} \text{min}^{-1}$) from Beehive to West Fork, respectively (Table 4, Figure 2.6 A). There was not a significant relationship between increased $[\text{NO}_3\text{-N}]$ (neither ambient nor average annual) and increased U_{amb} (p-values = 0.86 and 0.90, respectively, Tables 2 and 4, Figure 2.6 E). When comparing the two stream pairs (Beehive-Pony and North Fork-Upper Middle Fork), we found that the two streams (within each pair) with lower $[\text{NO}_3\text{-N}_{amb}]$ had smaller U_{amb} . Beehive's U_{amb} was 9.99 ($\mu\text{g m}^{-2} \text{min}^{-1}$) and North Fork's U_{amb} was 26.63 ($\mu\text{g m}^{-2} \text{min}^{-1}$) and the two higher $[\text{NO}_3\text{-N}_{amb}]$ (Pony and Upper Middle Fork) had U_{amb} values of 56.19 and 75.17 ($\mu\text{g m}^{-2} \text{min}^{-1}$), respectively (Table 4, Figure 2.6 E). The two non-paired streams had higher U_{amb} values than the other four streams, Lower Middle Fork was 215.63 ($\mu\text{g m}^{-2} \text{min}^{-1}$) and West Fork was 232.43 ($\mu\text{g m}^{-2} \text{min}^{-1}$) (Table 4, Figure 2.6 E).

Ambient uptake velocities (V_{f-amb}) did not have a significant relationship with either ambient or average annual $\text{NO}_3\text{-N}$ concentrations (Figure 2.5). Beehive, Upper Middle Fork, North Fork and Lower Middle Fork all had similar ambient uptake efficiencies (V_{f-amb}) ranging from 4.49 to 4.99 (mm min^{-1}) with a range in $[\text{NO}_3\text{-}N_{amb}]$ from 2.00 to 43.6 ($\mu\text{g l}^{-1}$) and average annual $\text{NO}_3\text{-N}$ concentrations from 20.8 to 213 ($\mu\text{g l}^{-1}$). For the two stream pairs (Beehive-Pony and North Fork-Upper Middle Fork), the stream reaches with lower $[\text{NO}_3\text{-}N_{amb}]$ (Beehive and North Fork) had greater ambient uptake efficiencies (larger V_{f-amb}), although the North Fork and the Upper Middle Fork were similar (Table 4). Pony, the smallest (both WA and Q) stream but the highest $[\text{NO}_3\text{-}N_{amb}]$ (68.3 $\mu\text{g l}^{-1}$) and second highest average annual $\text{NO}_3\text{-N}$ concentration (202 $\mu\text{g l}^{-1}$), had the lowest V_{f-amb} (0.82 mm min^{-1}). West Fork, the largest (both WA and Q) stream but the second lowest $[\text{NO}_3\text{-}N_{amb}]$ (3.96 $\mu\text{g l}^{-1}$) and third highest average annual $\text{NO}_3\text{-N}$ concentration (132 $\mu\text{g l}^{-1}$), had the highest V_{f-amb} by an order of magnitude (58.69 mm min^{-1}) (Tables 2 and 4).

$\text{NO}_3\text{-N}$ Spiraling Parameters from Constant-rate Additions (Plateau Approach)

Constant-rate additions were conducted in two of the six stream reaches, Beehive and Lower Middle Fork. Two constant-rate additions were conducted in Beehive (one with a lower and one with a higher $[\text{NO}_3\text{-}N]$ addition) and only one in Lower Middle Fork. Of these three experiments, only one of the experiments at Beehive (higher added $[\text{NO}_3\text{-}N]$) yielded a significant p-value for the regression of longitudinal data used to determine $S_{w-add-plateau}$ (p-value < 0.0001 for the higher $[\text{NO}_3\text{-}N]$ addition and p-value =

0.1474 for the lower [NO_3-N] addition) and the one on the Lower Middle Fork did not yield a significant relationship (p-value = 0.3760) (Table 5). We calculated an $S_{w-add-plat}$ for all three experiments despite having only one experiment yield a significant relationship. The two $S_{w-add-plat}$ values in Beehive were 2534 and 4140 (m) and Lower Middle Fork was 3483 (m) (Table 5). In Beehive, the $U_{tot-plat}$ values were 54 and 141 ($\mu\text{g m}^{-2} \text{min}^{-1}$) and at Lower Middle Fork $U_{tot-plat}$ was 788 ($\mu\text{g m}^{-2} \text{min}^{-1}$) (Table 5). In Beehive, the constant-rate addition (plateau approach) areal uptake rate value ($U_{tot-plat}$) for the higher added [NO_3-N] addition fell within the 95% confidence intervals (C.I.) for [$NO_3-N_{tot-dyn}$] versus $U_{tot-dyn}$ (Figure 2.7 A). The $U_{tot-plat}$ value for the lower added [NO_3-N] addition fell just outside the 95% C.I. (Figure 2.7 A). The $U_{tot-plat}$ value for the Middle Fork fell near the 95% C.I. (Figure 2.7 E). The $V_{f-tot-plat}$ values for the lower and higher [NO_3-N] additions at Beehive were 2.38 and 1.37 (mm min^{-1}) and the one addition at Lower Middle Fork was 1.53 (mm min^{-1}).

NO₃-N Spiraling Parameters Calculated through BTC-integration

We calculated NO₃-N spiraling parameters using the BTC-integrated approach for comparison between values calculated with the newly developed *TASCC* method and previously developed methods (i.e., plateau approach). Across the six stream reaches, $S_{w-add-int}$ ranged from 1115 m in West Fork to 2753 m in Beehive (Table 6). Although the longest $S_{w-add-int}$ was only ~ 2.5 times longer than the shortest, $V_{f-tot-int}$ varied by two orders of magnitude across the six sites. The lowest $V_{f-tot-int}$ was measured in Beehive (2.31 mm min^{-1}) and the highest in Pony (168 mm min^{-1}) (Table 6). The $U_{tot-int}$ varied by

four orders of magnitude, with the lowest $U_{tot-int}$ measured in Pony ($0.349 \mu\text{g m}^{-2} \text{min}^{-1}$) and the highest in West Fork ($4155 \mu\text{g m}^{-2} \text{min}^{-1}$) with each of the $U_{tot-int}$ values falling within or near the 95% C.I. for $[NO_3-N_{tot-dyn}]$ versus $U_{tot-dyn}$ (Table 6 and Figure 2.7).

Total NO_3 -N Uptake Parameters and M-M kinetics

We used the hyperbolic relationships between $[NO_3-N_{tot-dyn}]$ and $U_{tot-dyn}$ to parameterize the M-M kinetic model and estimate half-saturation constants (K_m) and maximum areal uptake rates (U_{max}) for each of our stream reaches. Data from all six reaches yielded significant fits to the M-M model (Figures 2.6 and 2.7); however, other kinetic models could be more appropriate in different systems (Dodds et al. 2002). For U_{max} , we again compared the two stream pairs (Beehive-Pony and North Fork-Upper Middle Fork), and found that the two streams in the pair of medium sized streams (North Fork and Upper Middle Fork) had greater U_{max} values than the two streams of the small pair (Beehive and Pony). North Fork had a U_{max} value of $456 (\mu\text{g m}^{-2} \text{min}^{-1})$ and Upper Middle Fork had a U_{max} value of $4820 (\mu\text{g m}^{-2} \text{min}^{-1})$, whereas, Beehive and Pony had U_{max} values of 197 and $357 (\mu\text{g m}^{-2} \text{min}^{-1})$, respectively (Table 4). Further, the stream reaches with lower $[NO_3-N_{amb}]$, Beehive and North Fork, had smaller U_{max} values and the two reaches with higher $[NO_3-N_{amb}]$, Pony and Upper Middle Fork, had larger U_{max} values (Table 4). The highest U_{max} , $10874 (\mu\text{g m}^{-2} \text{min}^{-1})$, was measured in the largest stream (West Fork). The two stream reaches within each pair that had lower $[NO_3-N_{amb}]$ had smaller K_m values (Tables 4). The K_m values for the two largest streams fell between the K_m values for the lower and higher $[NO_3-N_{amb}]$ streams within each pair (Table 4).

The shape of the M-M model fit curves varied for each of the six stream reaches. Streams with lower K_m values appear to move from U_{amb} to U_{max} more rapidly, i.e., the vertical section of the M-M model fit is steeper and has a more abrupt (or sharp) curve moving toward K_m and U_{max} than do curves with higher K_m values. As K_m values for the six stream reaches increased, the M-M model fit lines became more gradual and the curves became less abrupt (Figure 2.8). For Beehive ($K_m < 200$), the M-M model fit was steep approaching K_m and had the sharpest curve (Figure 2.8). For experimental stream reaches with $100 < K_m < 200$ (including: North Fork, Lower Middle Fork, and West Fork), the M-M model fit was less abrupt (Figure 2.8). At Pony and Upper Middle Fork ($K_m > 200$), the M-M model fits were rounder and more gradual and were not as steep as they approached K_m (Figure 2.8).

All of the $V_{f-tot-dyn}$ values for the six reaches are plotted against $[NO_3-N_{tot-dyn}]$ in Figure 2.9 A. The lowest $V_{f-tot-dyn}$ value for West Fork (28.8 mm min^{-1}) was nearly three times higher than the largest $V_{f-tot-dyn}$ value for any other stream (10.9 mm min^{-1}). For the two sets of stream pairs, the $V_{f-tot-dyn}$ values ranged from $1.28 - 10.9 \text{ (mm min}^{-1})$ and the highest $V_{f-tot-dyn}$ value for Pony was nearly half as large as the lowest value for the pairs. For comparison of $V_{f-tot-dyn}$ minima values, a hyperbolic decay model was fit to the six reaches; only five of the six stream reaches (excluding West Fork) are presented (Figure 2.9 B). Beehive and North Fork approach $V_{f-tot-dyn}$ minima at lower $[NO_3-N_{tot-dyn}]$ values than do Upper Middle Fork and Lower Middle Fork (Figure 2.9 B).

Seasonal Variation in NO₃-N
Retention and Uptake Dynamics

Across the seasonal tracer addition experiments in Beehive, discharge (Q) varied by two orders of magnitude. The lowest seasonal Q was measured in March 2009 (0.003 m³ s⁻¹) and greatest seasonal Q was measured in July 2008 (0.137 m³ s⁻¹) (Table 2 and Figure 2.10 A).

Total, physical, and biological retention of added NO₃-N also varied across seasons in Beehive. The summer experiment (July 2008) had the greatest biological NO₃-N retention (11%) and the lowest for both physical (42%) and total (53%) retention of added NO₃-N (Table 3 and Figure 2.10 B). The greatest physical retention (89%) was measured in March 2009 and the lowest biological retention (1.5%) was measured in October 2006. (Table 3 and Figure 2.10 B). The greatest total NO₃-N retention occurred during the March (winter) experiments, decreased during the October (fall) experiments, and was lowest during the July (summer) experiment (Figure 2.10 B). From this headwater stream reach, 53 – 92% of the NO₃-N added during the five seasonal experiments was retained; therefore over the timescale of each experiment 8 – 47% was exported downstream, depending on the season.

Ambient uptake parameters also varied across seasons. S_{w-amb} ranged from 171 – 1589 m. The shortest S_{w-amb} was measured in October 2006 and the longest was measured in March 2009. The lowest U_{amb} was measured in October 2007 and the highest was in October 2006, 5.61 and 14.25 (μg m⁻² min⁻¹) respectively. October 2006 yielded the highest measured V_{f-amb} (7.81 mm min⁻¹) and the lowest was in March 2009 (0.12 mm min⁻¹) (Table 4). The BTC was measurable (we measured a change in Cl and

$\text{NO}_3\text{-N}$ concentrations) during the March 2007 sampling event. However, the linear regression of $\text{NO}_3\text{-N}_{\text{tot-dyn}}$ concentration versus S_w used to calculate the $S_{w\text{-amb}}$ yielded a negative y-intercept (i.e., negative $S_{w\text{-amb}}$). Therefore, because the $S_{w\text{-amb}}$ value is used for calculating the other ambient uptake parameters but in this case was immeasurable, we were unable to calculate any ambient uptake parameters for the March 2007 experiment.

Across seasons in Beehive, the longest $S_{w\text{-add-int}}$ was approximately four times longer than the shortest (1225 m in March 2007 and 5081 m in October 2006) (Table 6). The $U_{\text{tot-int}}$ varied by two orders of magnitude, the lowest $U_{\text{tot-int}}$ was measured in March 2007 ($3.90 \mu\text{g m}^{-2} \text{min}^{-1}$) and the highest in July 2008 ($110 \mu\text{g m}^{-2} \text{min}^{-1}$) (Table 6 and Figure 2.11). The $V_{f\text{-tot-int}}$ values across seasons also varied by two orders of magnitude. The lowest $V_{f\text{-tot-int}}$ was measured in March 2009 (0.070mm min^{-1}) and the highest in July 2008 (2.31mm min^{-1}).

For the seasonal instantaneous tracer addition experiments conducted at Beehive, the M-M hyperbolic regressions for calculating U_{max} were only significant for three of the five experiments, July 2008, March 2009, and October 2007 (p-values ≤ 0.0001) (Table 4 and Figure 2.11). For these three experiments, U_{max} was greatest in July ($197 \mu\text{g m}^{-2} \text{min}^{-1}$) and lowest in March ($88 \mu\text{g m}^{-2} \text{min}^{-1}$), while the lowest significant K_m was measured in July ($23.2 \mu\text{g l}^{-1}$) and the highest in the March 2009 ($689.8 \mu\text{g l}^{-1}$) (Table 4 and Figure 2.10 C).

The general shapes of the parameterized M-M model varied across the five seasonal experiments conducted in Beehive. Seasons with higher K_m values indicated that uptake adjusted more slowly from U_{amb} to U_{max} with increased $[\text{NO}_3\text{-N}]$ than do

seasons with lower K_m values (Figure 2.11 F). For seasons with $K_m < 100$ (including: July 2008, October 2006 and March 2007), the M-M models were more abrupt and were steeper than other seasons while approaching K_m (Figure 2.11 F). For October 2007 ($K_m = 135$), the M-M model had a rounder, more gradual curve approaching K_m than seasons with $K_m < 100$. The M-M model for March 2009 ($K_m > 200$) had the most gradual curve and was not as steep while approaching K_m (Figure 2.11 F).

The $V_{f-tot-dyn}$ values that represent nutrient uptake efficiency ranged from a minimum of $0.057 \text{ (mm min}^{-1}\text{)}$ in March 2009 to a maximum of $10.9 \text{ (mm min}^{-1}\text{)}$ in July 2008 (Figure 2.12 A). The hyperbolic decay model fits are shown for four of the five reaches, March 2007 was excluded because the model fit was not significant ($p\text{-value} = 0.9743$) (Figure 2.12 B). The $V_{f-tot-dyn}$ values for March 2009 were not much greater than the minima. July 2008 reached a $V_{f-tot-dyn}$ minima value at a higher $[NO_3-N_{tot-dyn}]$ than the other seasons (Figure 2.12 B).

Results Summary

In summary, watershed area, discharge, stream order, number of structures per watershed, seasonality, and $[NO_3-N_{amb}]$ influenced nutrient retention and uptake dynamics (Figures 2.3, 2.5, 2.9, and 2.11). For the six sites studied in the West Fork Gallatin Watershed, physical $NO_3\text{-N}$ retention generally decreased as watershed area increased and biological $NO_3\text{-N}$ retention increased as watershed area increased (Figure 2.4 A and B). At Beehive, $NO_3\text{-N}$ retention varied across seasons, however the patterns were not as clear (Figure 2.10 B). The highest proportion of biological retention and

lowest total retention occurred in July; total retention increased during October and was highest during the March experiments (Table 3 and Figure 2.10 B).

Ambient uptake lengths across the six sites varied with ambient conditions. For the four larger stream reaches, S_{w-amb} decreased as watershed area increased (Tables 2 and 4). S_{w-amb} generally decreased as both discharge and stream order increased for five of the six sites. Streams reaches with increased $[NO_3-N_{amb}]$ generally had decreased S_{w-amb} values; however, West Fork did not fit this trend (Table 4 and Figure 2.5). We observed a general decrease in S_{w-amb} with an increase in average annual NO_3-N concentration for all six sites (p-value = 0.03, $r^2 = 0.72$) and between site pairs (Figure 2.5). For the Beehive experiments, seasonality influenced S_{w-amb} ; it was lowest during the fall experiments and greatest during one of the winter experiments (March 2009) (Table 4).

Watershed area, stream order and number of structures had a significant influence on ambient areal uptake rates (U_{amb}) across the six reaches (p-values = 0.03, 0.04, and 0.0001, respectively and $r^2 = 0.72$, 0.70, and 0.98, respectively) (Figure 2.6 A, B, and D). For U_{max} , watershed area and discharge both had significant positive correlations (Figure 2.6 F and H). At Beehive, U_{amb} , U_{max} , and K_m all varied across seasons, but specific temporal patterns were difficult to discern (Figure 2.10 C).

For both the spatial and seasonal tracer addition experiments, the $U_{tot-dyn}$ values fell within or near the 95% confidence intervals (C.I.) (Figures 2.6 and 2.10). Most of the $U_{tot-int}$ values fell within the 95% C.I., while some of them were near the limit. The three $U_{tot-plat}$ values fell within or just outside of the 95% C.I. (Figures 2.6 A and E and 2.10 D).

The shape of the M-M model indicates the rate of change in $U_{tot-dyn}$ with changes in $[NO_3-N]$. Across the six sites and the five seasons, as K_m values increased, M-M models were less abrupt (i.e., the curves were more gradual) (Figures 2.7 and 2.10 F). For sites and seasons with $K_m < 100$, the M-M model fits were steeper as they approached K_m values (Figure 2.8 and 2.10 F). For sites and seasons with $100 < K_m < 200$, the M-M were less abrupt (more gradual). The M-M model fit for $K_m > 200$ had a rounder, more gradual curve.

Ambient uptake velocity (V_{f-amb}) values were quite similar for four of the six streams (Beehive, Upper Middle Fork, North Fork and Lower Middle Fork) despite other ambient conditions varying across these four sites (Table 4); the relationship between total dynamic uptake efficiency ($V_{f-tot-dyn}$) and $[NO_3-N_{tot-dyn}]$ varied across sites (Figure 2.9 A and B). For the seasonal experiments at Beehive, V_{f-amb} varied across seasons, but the $V_{f-tot-dyn}$ minima were highest for increasing $[NO_3-N_{tot-dyn}]$ during the July experiment and lowest during the March 2009 experiment (Figure 2.12 A and B).

Discussion

How Do Stream Uptake Kinetics and Spiraling Parameters Vary across Streams of Different Development Intensity and Scale?

Assessment of Watershed Size (Watershed Area and Discharge) and Nitrate

Concentration Influences on Uptake Kinetics: Most research on stream NO_3-N retention and uptake dynamics to date has been performed at the single reach-scale (e.g., Dodds et al. 2002, Ensign and Doyle 2006, O'Brien et al. 2007, Mulholland et al. 2008, Hall et al.

2009) and only recently have experiments in large rivers (e.g., Tank et al. 2008) or across stream networks (e.g., Covino et al. 2010) been undertaken. We sought to conduct a watershed-scale study across a range of stream reach types, flow states, seasons, and ambient nutrient concentrations to improve understanding of $\text{NO}_3\text{-N}$ retention and uptake dynamics across a stream network. Although each experiment was performed in a single reach, experiments were conducted along six reaches across the watershed that varied in stream order, watershed area (WA), discharge (Q), and ambient nutrient conditions. Most watershed-scale modeling studies have employed single or a few reach-scale data sets to predict how a stream network (Alexander et al. 2009) or region might respond to increases in nutrient loading (Boyer et al. 2006). Here, we seek to improve understanding of $\text{NO}_3\text{-N}$ retention and transport across a stream network to assess physical nitrate retention and biological nitrate uptake kinetics across space and time.

We calculated total, physical, and biological retention of added $\text{NO}_3\text{-N}$ and uptake kinetics across six reaches. Biological spiraling metrics included uptake lengths (S_w), uptake velocities (V_f), and areal uptake rates (U) across broad ranges of concentration from ambient to nitrogen saturation. Ambient uptake length ($S_{w\text{-amb}}$) was not significantly correlated to scale (WA and Q) (p-value > 0.05), but without Pony, $S_{w\text{-amb}}$ for the remaining five stream reaches decreased significantly as WA increased (p-value = 0.04, $r^2 = 0.80$). Pony was the smallest stream studied (both WA and Q) but had the highest $[\text{NO}_3\text{-N}_{\text{amb}}]$. These results suggest that WA was a good indicator of $S_{w\text{-amb}}$, except in a small watershed with elevated $[\text{NO}_3\text{-N}_{\text{amb}}]$. Pony is a headwater stream whose watershed and stream corridor have been heavily disturbed (with ski lifts, parking

lots, and more than 100 structures contributing to the small 0.901 km² watershed). Comparable but undisturbed adjacent watersheds exhibited low or undetectable (< 2.0 μg l⁻¹) stream [NO₃-N] (Gardner and McGlynn 2009). Five of the six reaches (excluding West Fork) exhibited significant decreased S_{w-amb} with increased [NO₃-N_{amb}]. For all six reaches increased average annual [NO₃-N] was significantly correlated to a decrease in S_{w-amb} (Figure 2.5 A). The West Fork has the largest WA and exhibited the second lowest [NO₃-N_{amb}], and was therefore consistent with the WA versus S_{w-amb} inverse relationship, but not the observed relationship between decreased S_{w-amb} and increased [NO₃-N_{amb}]. The West Fork has the third largest average annual [NO₃-N] suggesting that although [NO₃-N_{amb}] was low at the time of the experiment, the biological community was likely well developed due to a history of nutrient loading and higher concentrations. Therefore, the West Fork had a shorter ambient spiraling length (S_{w-amb}) than one would expect solely based on the [NO₃-N_{amb}] from the day of the experiment. Although we did not measure biological communities, through in-field observations we saw growth in populations of algae and other macrophytes in the streams with both elevated [NO₃-N] and in streams lower in the watershed (i.e., larger streams with greater stream bed area). Chronic increased [NO₃-N] in a system that remains N limited could result in a more productive biological community and therefore increased ambient uptake (i.e. shorter S_{w-amb} values), until it begins to exhibit NO₃-N saturation characteristics (Dodds et al. 2002, Earl et al. 2006) or co-limitation (Elser et al. 2007, Sanderson et al. 2009).

These results are not consistent with the general paradigm of increased Q leading to increased S_{w-amb} (e.g., Valett et al. 1996, Butturini and Sabater 1998) nor increased

ambient N leading to increased S_w (Mulholland et al. 2008) and suggest that these systems are still N limited (Earl et al. 2006). Our results also suggest that longer time integration of streamwater concentrations rather than instantaneous ambient concentration are important for assessment of uptake dynamics and that other variables can overwhelm the influence of Q on S_{w-amb} . Further, S_{w-amb} was not necessarily a good indicator for overall capacity of a stream reach to retain increased NO_3-N loads (i.e., S_{w-amb} were not highly correlated to U_{max} nor K_m values). Additionally, it should be noted that our results represent inter-stream comparisons despite their locations within the same larger stream network and therefore represent fundamentally different observations than manipulating concentration in one reach (Mulholland et al. 2002, Covino et al. 2010). This is an important point as syntheses of stream tracer experiments attempt to use inter-stream comparison to develop global relationships between spiraling metrics and concentration when they are problematic even within the same network due to strong differences in variables such as biological community assemblage, metabolism, nutrient stoichiometry, light availability, antecedent nutrient dynamics, and hydrologic setting. We attempted to control for as many variables as possible, but there are inherent uncontrollable differences, even within individual stream reaches.

Uptake length (S_w) is often normalized to uptake velocity (V_f) or areal uptake rate (U) to enable comparison between stream reaches and seasons to account for differences in stream Q , velocity, depth, and streambed area (Stream Solute Workshop 1990, Davis and Minshall 1999, Dodds et al. 2002). We calculated U_{amb} and V_{f-amb} for each stream reach. Unlike S_{w-amb} , U_{amb} was significantly correlated to WA for all six stream reaches,

U_{amb} increased with greater WA (Figure 2.6 A). There was not a significant relationship between either U_{amb} and Q nor U_{amb} and $[NO_3-N_{amb}]$ across stream reaches (Figure 2.6 C and E). It has been suggested that V_{f-amb} decreases with increasing N loads within a stream network (Wollheim et al. 2008). Based on this, we might expect to see a decrease in V_{f-amb} with an increase in $[NO_3-N_{amb}]$; V_{f-amb} values for Pony and West Fork were consistent with this, yet the other four streams were not. However, inter-stream comparisons are challenging because many variables in addition to ambient nutrient concentration change between sites, complicating simple comparisons as described above and previously (Covino et al. 2010). V_{f-amb} was similar for four of the six streams, with values at Beehive, North Fork, Upper Middle Fork, and Lower Middle Fork ranging from 4.49 to 4.99 ($mm\ min^{-1}$) despite large ranges in WA ($5.7 - 83.4\ km^2$), Q ($0.137 - 0.311\ m^3\ s^{-1}$), and $[NO_3-N_{amb}]$ ($2.00 - 43.6\ \mu g\ l^{-1}$) (Tables 2 and 4 and Figure 2.5). These four streams have similar ambient uptake efficiencies, indicated by V_{f-amb} , but respond differently to increases in $[NO_3-N]$. The shapes of the $V_{f-tot-dyn}$ curves (rates at which V_f decreases with increasing $[NO_3-N]$) differ with increases in stream $[NO_3-N]$ (Figure 2.9), uptake efficiencies in streams with lower $[NO_3-N]$ decrease more rapidly. This suggests that uptake efficiency decreases more slowly in streams that have experienced greater past loading than in pristine streams in response to further increases in concentration.

U_{max} values had significant positive relationships with both WA and Q , but not with $[NO_3-N_{amb}]$ (Figure 2.6). U_{max} was greatest at the bottom of the watershed (West Fork experimental reach, which has the greatest WA), where development first started and is most intense. Since development started in the West Fork Gallatin Watershed,

both the number of structures and $[\text{NO}_3\text{-N}]$ show a strong increasing trend with time (Figure 2.2). Kaushal et al. (2006) saw similar trends of both structures and $[\text{NO}_3\text{-N}]$ increasing with time in a snowmelt dominated, developing mountain watershed in Colorado. In the West Fork Gallatin Watershed, increases in $[\text{NO}_3\text{-N}]$ may have encouraged algal and microbial community growth and therefore greater potential for biologic retention. So, although the $[\text{NO}_3\text{-N}]$ was not as high as one would expect given the U_{max} measured at the watershed outlet, the WA does fit the trend of increasing U_{max} with increasing stream size and $[\text{NO}_3\text{-N}]$ has increased since development started. The half-saturation constant (K_m) values can be a good indicator of stream reach response to increases in $[\text{NO}_3\text{-N}]$. Streams with smaller K_m values indicate that they will likely have a more rapid uptake response to increases in $[\text{NO}_3\text{-N}]$ and therefore could retain more $\text{NO}_3\text{-N}$ in response to increasing short term $\text{NO}_3\text{-N}$ loads than stream with higher K_m values. However in the streams we analyzed, K_m values did not show significant relationships with scale (WA and Q) nor $[\text{NO}_3\text{-N}_{\text{amb}}]$ or average annual $[\text{NO}_3\text{-N}]$. This suggests that while although K_m is a valuable stream metric for assessing uptake capacity in response to increased short term nutrient loading; it is not easily predictable given current stream ecosystem understanding. A greater understanding of stream conditions (i.e., stream productivity, benthic stoichiometry data, etc.) would increase understanding of a stream's ecosystem and in turn potentially increase predictability.

Predicting or attributing $\text{NO}_3\text{-N}$ retention and uptake magnitudes in stream reaches is difficult due to the multiple drivers influencing these dynamics. Some studies have suggested that ambient nutrient concentration is the main driver for nutrient

retention or uptake (e.g., Mulholland et al. 2008) while others suggest the greatest driver is Q (e.g., Valett et al. 1996, Butturini and Sabater 1998). Our data generally suggest that uptake metrics increase in magnitude with increasing WA , stream order, Q , number of structures, ambient nitrate, and average annual nitrate (which are themselves correlated to one another to varying degrees). However, these general trends are often not followed by one or more individual reaches of the six described herein. We suggest that this occurs because of the multitude of factors and feedbacks between them including but not limited to: WA , stream order, number of structures per watershed, seasonality, average annual $[NO_3-N]$, hyporheic exchange, stream morphology, biologic communities, metabolism, and antecedent conditions all influence NO_3-N retention and uptake dynamics to varying degrees in space and time. Despite these stream reaches all located across one stream network, the spatial expanse was large and these analyses still represent inter-stream comparisons where many variables in addition to ambient nutrient concentration change among sites, complicating simple comparisons (Covino et al. 2010). The complexity and lack of simple relationships to ambient spiraling parameters and even more sophisticated uptake kinetic model parameters across one stream network suggest that global relationships across regions might remain elusive or at least exhibit a high degree of scatter given current metrics and understanding. However, while imperfect we did find general trends which relate these variables (Q , WA , $[NO_3-N_{amb}]$) to nutrient retention spiraling parameters and suggest that our quantification of dynamic uptake behavior in response to changing concentration sheds new light on the dynamics of nutrient spiraling and uptake kinetics across space and time.

Assessment of Uptake Kinetic Model Shapes: Michaelis-Menten (M-M) kinetic models are traditionally used to model enzyme kinetics. In the mid-1960s, researchers focused on nutrient limitation and algal growth began using similar methods to determine nutrient uptake parameters (Dugdale 1967). Current use of M-M hyperbolic relationships to determine nutrient uptake dynamics is not uncommon (Dodds et al. 2002, Earl et al. 2006, Newbold et al. 2006, Covino et al. 2010, Covino et al. in press). Uptake potential (or responsiveness to increasing concentration or load) can be estimated by the shape of the M-M or other appropriate kinetic model as well as the magnitude of U_{\max} (for the M-M kinetic model). Stream reaches with steep M-M kinetic models were more responsive to changes in $\text{NO}_3\text{-N}$ concentrations (e.g. Beehive and West Fork). Stream reaches that are more responsive have lower K_m values, arrive at U_{\max} at a lower $[\text{NO}_3\text{-N}]$, and attain higher uptake efficiency at lower $[\text{NO}_3\text{-N}]$ than the streams with more gradual response. For the six stream reaches studied in the West Fork Gallatin Watershed, K_m did not have a significant relationship with stream size (WA or Q) or $[\text{NO}_3\text{-N}]$ (ambient or average annual); therefore curve shape cannot be easily attributed to $[\text{NO}_3\text{-N}]$ (ambient or average annual) or watershed size (WA or Q). Despite lack of correlation to ambient concentration or other simple variables, assessment of kinetic model shape does provide insight into stream reach uptake potential and retention behavior in response to transient changes in stream concentration and therefore retention capacity (Covino et al. 2010).

Earl et al. (2006) utilized uptake – concentration curve shape to categorize stream nutrient saturation state. When compared to the Saturation Response Types defined by Earl et al. (2006), the six stream reaches studied in the West Fork Gallatin Watershed

would be primarily Saturation Response Types (SRT) I (well below nutrient saturation – Beehive, Upper Middle Fork, North Fork, and West Fork) and II (approaching nutrient saturation – Pony and Lower Middle Fork) and none of the streams exhibited a SRT III (nutrient-saturated stream). Our analyses and those of Earl et al. (2006) suggest that uptake versus concentration curves are useful tools for assessing stream nutrient status and behavior and that in addition to response types, appropriate kinetic parameters are useful metrics of stream nutrient status.

Currently, the six stream reaches studied in the West Fork Gallatin Watershed appear to be adjusting to increases in development and $\text{NO}_3\text{-N}$ loading. $\text{NO}_3\text{-N}$ concentrations are elevated in some streams an order of magnitude above background and this suggests shifts in uptake – concentration behavior as ascertained by paired stream comparison (Figure 2.7). However, none of the streams analyzed appear to be $\text{NO}_3\text{-N}$ saturated. As development and increases in $\text{NO}_3\text{-N}$ loading continue, the streams may shift and exhibit saturation behavior. However, adjustments of biological communities, productivity, metabolic processes, and other limiting nutrients should be considered to improve understanding of stream ecosystem response to increased nutrient loading, not only across the stream network, but across seasons as well.

How do Uptake Kinetics and Spiraling Parameters Vary across Season in a Snow Dominated Mountain Stream?

Both ambient and maximum areal uptake rates (U_{amb} and U_{max}) have been shown to increase with stream size (WA and Q) in the six stream reaches studied in the West Fork Gallatin Watershed. Seasonality can also influence $\text{NO}_3\text{-N}$ retention and uptake

dynamics. Influencing seasonal factors in snow dominated mountain watersheds include, but are not limited to: annual shifts in ambient $\text{NO}_3\text{-N}$ concentrations and stream loading, Q , temperature, available photosynthetically active radiation, other biologically active nutrient concentrations (e.g., C , PO_4), and antecedent conditions. In addition, stream biomass standing stocks and whole stream metabolism (Simon et al. 2005), which are also sensitive to seasonality in driving variables, may be primary drivers of temporal variation of nutrient retention and uptake dynamics.

Temporal studies have been conducted in streams with moderate seasonality (e.g., Simon et al. 2005) relative to snowmelt dominated mountain systems, however winter tracer addition experiments are logistically challenging and we are not aware of other field based studies in strongly seasonal systems such as the West Fork Gallatin Watershed. However, seasonal stream chemistry data has been widely collected and models have been used to predict seasonal retention and uptake dynamics (e.g., Alexander et al. 2009). In the Western U.S. and other seasonally snow-covered watersheds, $[\text{NO}_3\text{-N}]$ are often highest in the winter, prior to peak snowmelt and lower during peak biological potential in the summer (Williams et al. 1996, Sickman and Melack 1998, Gardner and McGlynn 2009).

Across the West Fork Gallatin Watershed from September 2005 through September 2007, peak $[\text{NO}_3\text{-N}_{\text{amb}}]$ were observed during winter months, before peak snowmelt runoff began (Gardner and McGlynn 2009). Creed and Band (1998) observed higher $[\text{NO}_3\text{-N}_{\text{amb}}]$ on the rising limbs of the snowmelt hydrograph and suggested that $\text{NO}_3\text{-N}$ was being flushed out of soil pores with snowmelt runoff. Like Creed and Band

(1998), at West Fork Gallatin Watershed we observed highest $\text{NO}_3\text{-N}$ values during winter, but it was during baseflow before peak snowmelt began. The intersection of stream nutrient concentration seasonality with stream nutrient uptake seasonality has strong implications for the potential of in-stream nutrient retention to alter downstream loading and watershed export. The vast majority of stream nutrient release experiment's spiraling assessments have been conducted during summer baseflow when uptake is arguably at its highest levels while stream network nutrient transport is at its lowest. This has strong implications for the role of in-stream retention on annual watershed nutrient export and parameterization of annual models for stream network transport of retained nutrients. Specifically, in-stream retention can be overestimated or misestimated as one attempts to scale measures of stream nutrient retention in time and across seasons.

Here we assess stream $\text{NO}_3\text{-N}$ spiraling and uptake kinetics across five seasons in the Beehive study reach (Table 4 and Figures 2.9, 2.10, 2.11). U_{amb} values varied relatively little across the five seasons measured in Beehive, and ranged from 5.61 – 14.2 ($\mu\text{g m}^{-2} \text{min}^{-1}$) (Table 4 and Figure 2.10 C). This suggest that U_{amb} values vary little within this stream reach perhaps because biological communities (algae, microbes, etc.) exist and process nutrients year round in this system, though their ability to process increased $\text{NO}_3\text{-N}$ loads did vary more strongly across seasons. Maximum areal uptake rates (U_{max}) and half saturation constants (K_m) varied strongly across seasons. For the three seasons that had significant M-M kinetic model fits, U_{max} ranged from 88 – 197 ($\mu\text{g m}^{-2} \text{min}^{-1}$) and K_m ranged from 23 – 690 ($\mu\text{g l}^{-1}$) (Table 4 and Figure 2.10 C). U_{max} was highest in the summer; this is likely attributed to increased biomass, photosynthesis,

temperature, and metabolic processes that occur when there is more available sunlight and warmer stream temperatures. The K_m for this reach was lowest in the summer, which indicates that the stream reach was more responsive to increases in $[\text{NO}_3\text{-N}]$, thus reaching maximum uptake capacity at lower $[\text{NO}_3\text{-N}]$ and thus able to retain more $\text{NO}_3\text{-N}$. The two winter experiments yielded different kinetic model parameters with Winter 2007 experiments yielding greater U_{max} and K_m although the Winter 2007 experiment was conducted during a thaw that resulted in open stream conditions, warmer temperatures, lower $[\text{NO}_3\text{-N}_{\text{amb}}]$, and strong radiation inputs than contrasted with the Winter 2009 experiments that were conducted during more typical cold winter, snow covered stream conditions with a higher $[\text{NO}_3\text{-N}_{\text{amb}}]$. Our results indicate general seasonality in $\text{NO}_3\text{-N}$ uptake dynamics and efficiency (Figures 2.10 and 2.11) with decreases during colder lower radiation times of the year. However within a given season the magnitude of uptake response to concentration can vary strongly as evidenced by repeat experiments in March and October which suggest responsiveness to short term changes in conditions.

These seasonal experiments indicate that U_{max} was greatest in the summer and least in the winter, showing distinct seasonality (Figure 2.10 C) suggesting that Beehive could retain more $\text{NO}_3\text{-N}$ from the water column in the summer than in the fall or winter. The shape of the uptake efficiency and kinetic model curves and M-M model parameterization in response to elevated concentrations were seasonally variable and indicated nutrient uptake was not limited to summer months and that ambient uptake alone is a poor predictor of seasonal nutrient retention capacity. These results have

implications for extrapolation of single point-in-time experiments across seasons or even within seasons as indicated by uptake kinetics variability documented here and suggest caution for assuming that short term experiments are reflective of longer term stream spiraling behavior.

What are the Relative Magnitudes of Stream Physical versus Biologic Retention of Added Nitrate across Streams from 1st to 4th Order?

Nitrate-N is retained from the water column through both physical (i.e. hydrologic) and biological (i.e. uptake) processes. We measured total retention of added NO₃-N across our six stream reaches in the West Fork Gallatin Watershed and across seasons in one of the experimental reaches (Beehive). We define total NO₃-N retention as the amount of NO₃-N added at the upstream endpoint of the experimental stream reach that is not measured at the downstream endpoint, which is the sum of physical and biological NO₃-N retention. Physical NO₃-N retention is hydrologic retention (e.g, water moving into the groundwater, hyporheic zones, etc.) that does not return to the experimental stream reach during the timeframe of the experiment. Nutrient solute that leaves the stream channel can be taken up biologically outside of the stream channel (e.g., riparian plant uptake) either on a short time scale or a longer time scale. After being stored for a period of time, it could return to the channel at some time point beyond the length of our study, or it could be stored long term in groundwater; all of which serve to increase stream reach nutrient retention and attenuate pulses of nutrient input (e.g., snow melt flushing events). Based on comparison of conservative tracer recovery in the same reach for both instantaneous and 6-10 hour constant-rate tracer addition

experiments, we determined that there was no systematic bias in recovery rates between the two experiment durations and we term physical retention as greater than ~12 hour duration (e.g., Covino et al. 2010). Biological $\text{NO}_3\text{-N}$ retention is the $\text{NO}_3\text{-N}$ retained from the water column through biological processes (e.g., $\text{NO}_3\text{-N}$ uptake). From the 1st to 4th order streams studied in the West Fork Gallatin Watershed, percent total, physical, and biological $\text{NO}_3\text{-N}$ retention of added $\text{NO}_3\text{-N}$ varied strongly across the watershed (Figure 2.4 A and B). Most past studies have focused solely on biologic uptake (i.e., biologic retention) and analyses based on recovered conservative and nutrient tracer alone; however physical retention can be a large portion of total retention and therefore should also be determined (Triska et al. 1989a, Claessens et al. 2009, Covino et al. 2010). It should be noted that nutrient retained by physical mechanisms could then also be biologically retained; however this is not quantifiable with current methods (Covino et al. 2010).

Across the six stream reaches studied in the West Fork Gallatin Watershed, there was a significant increase in biological retention of added $\text{NO}_3\text{-N}$ with increased watershed area (WA) and a significant decrease in physical retention of added $\text{NO}_3\text{-N}$ with increased WA (Figure 2.4 A and B). Claessens et al. (2009) found that $\text{NO}_3\text{-N}$ exports increased with increasing Q. Our results were consistent; we observed decreasing total retention with both increasing WA and Q, but neither relationship was statistically significant (p-value > 0.05) (Table 3). However, we did observe a statistically significant decrease in percent physical retention of added $\text{NO}_3\text{-N}$ with increasing WA (p-value = 0.002, $r^2 = 0.76$) (Table 3 and Figure 2.4 A). Mulholland et al.

(2008) suggested that both small and large streams can retain $\text{NO}_3\text{-N}$ efficiently, but for different reasons (stream bed area: water volume versus longer transport distance and increased residence times). In the 1st to 4th order streams in the West Fork Gallatin Watershed, we see similar results, but as WA increased there was a shift from more physical to more biological retention of added $\text{NO}_3\text{-N}$ (as the ratio of total retention of added $\text{NO}_3\text{-N}$). Our results suggest that physical and biological retention are both important mechanisms to consider as we model and assess nutrient retention across stream networks and assess the role of stream retention of nutrients in a watershed export context (Gardner and McGlynn 2009).

Percent total, physical and biological retention of added $\text{NO}_3\text{-N}$ also varied across seasons in the Beehive experimental reach. Total retention of added $\text{NO}_3\text{-N}$ was lowest in the summer (Figure 2.10 B) and physical (hydrological) processes dominated total $\text{NO}_3\text{-N}$ retention. Physical retention of added $\text{NO}_3\text{-N}$ was higher than biological retention of added $\text{NO}_3\text{-N}$ in the summer, but the ratio of biological to total $\text{NO}_3\text{-N}$ retention was greatest in summer. Biological uptake increased during summer months likely because there was an increase in photosynthesis with the increased hours of daylight and metabolic processes increase with increased stream temperatures. During summer months, Q is at or near baseflow and biological uptake potential can therefore most influence downstream concentrations and loading. Discharge was low during fall and winter but the biological uptake potential was lower due to decreased metabolic processing with low stream temperatures and decreased photosynthesis with minimal hours of sunlight combined with snow/ice cover across streams. During spring months,

the streams experience peak snowmelt conditions (peak annual Q) with water moving rapidly through the stream network (Wondzell et al. 2007) with less opportunity for NO₃-N retention or uptake while biological potential is low. We suggest that in addition to assessment of the relative magnitudes of physical and biological retention across stream sizes, seasonality should also be considered as we move toward watershed and stream network assessment of nutrient export and retention.

Summary

The West Fork Gallatin Watershed has seen a significant increase in development since the early 1970s. Nutrient concentrations in the watershed have also increased in association with this development. Retention and uptake dynamics of NO₃-N appear to be influenced by these elevated nutrient concentrations, but streams do not yet appear to be experiencing NO₃-N saturation.

How do stream uptake kinetics and spiraling parameters vary across streams of different development intensity and scale? Ambient NO₃-N concentrations in the West Fork Watershed have increased with escalated development over the last four decades. Our inter-stream comparison of S_{w-amb} in the West Fork Gallatin Watershed was not consistent with the general paradigm of increased Q leading to longer S_{w-amb} and elevated [NO₃-N_{amb}] leading to longer S_{w-amb} . This suggests that these systems are still N limited. However, for comparison of streams across a watershed, it can be more useful to compare uptake efficiency (V_f) or areal uptake rates (U_{amb} or U_{max}) as they are normalized for Q. Our results indicated that in pristine streams uptake efficiency ($V_{f-tot-dyn}$) decreased more

rapidly in response to additional increases in concentration than in streams that have experienced greater past loading. Further, U_{amb} increased with larger WA and we saw greater U_{max} with increases in both WA and Q, but neither U_{amb} nor U_{max} were significantly correlated to $[NO_3-N_{amb}]$. Although we did not measure biological communities, there was a visible growth in populations of algae and other macrophytes in the streams with both elevated $[NO_3-N]$ and in streams lower in the watershed (i.e., larger streams with greater stream bed area). Further research of biologic communities could inform what other major drivers of NO_3-N retention and uptake dynamics exist in the West Fork Gallatin Watershed and the feedbacks between loading, stream productivity, and enhanced nutrient uptake while nitrogen is still the limiting nutrient.

How do uptake kinetics and spiraling parameters vary across season in a snow dominated mountain stream? Annual shifts in ambient NO_3-N concentrations and stream loading, Q, temperature, available photosynthetically active radiation, concentrations of other nutrients (e.g., phosphorous), and antecedent conditions can lead to seasonal variability in nutrient retention and uptake dynamics. We observed the highest $[NO_3-N_{amb}]$ during winter months, and we conducted five experiments in one of the experimental stream reaches over a three-year period to examine seasonal variability in nutrient uptake. U_{amb} was relatively consistent across seasons suggesting uptake occurs year round with the capacity for uptake of elevated NO_3-N varying across seasons. The highest U_{max} values and lowest K_m values were measured during summer showing more rapid response to elevated $[NO_3-N]$ and increased capacity for increased NO_3-N

retention. Our results document the strong seasonal nature of nutrient retention and the variability possible within seasons to short-term response to environmental conditions.

What are the relative magnitudes of stream physical versus biologic retention of added nitrate across streams from 1st to 4th order? In West Fork Gallatin Watershed, biological retention of added NO₃-N increased with greater watershed area and physical retention of added NO₃-N decreased with greater watershed area. There was a substantial increase in biological retention of added NO₃-N as physical retention decreased. Physical retention typically comprised a larger proportion of total retention of added NO₃-N across seasons, but the highest ratio of biological to total retention occurred during summer indicating increased biological uptake during this time period. We suggest that both physical and biological nutrient retention need to be considered when analyzing stream network nutrient retention. Furthermore, we suggest that biological community adjustments should be considered to better understand stream ecosystem response to increased nutrient loading.

We suggest that quantifying physical and biological contributions to total retention and determining uptake kinetics from ambient to saturation over space, time, and development intensities can yield new insight into the capacity of stream networks to buffer nutrient loading. This work provides initial insight into the nature of the space – time heterogeneity of nutrient retention dynamics.

References Cited

- Alexander, R. B., J. K. Bohlke, E. W. Boyer, M. B. David, J. W. Harvey, P. J. Mulholland, S. P. Seitzinger, C. R. Tobias, C. Tonitto, and W. M. Wollheim. 2009. Dynamic modeling of nitrogen losses in river networks unravels the coupled effects of hydrological and biogeochemical processes. *Biogeochemistry* **93**:91-116.
- Bernhardt, E. S., G. E. Likens, D. C. Buso, and C. T. Driscoll. 2003. In-stream uptake dampens effects of major forest disturbance on watershed nitrogen export. *Proceedings of the National Academy of Sciences of the United States of America* **100**:10304-10308.
- Biggs, T. W., T. Dunne, and L. A. Martinelli. 2004. Natural controls and human impacts on stream nutrient concentrations in a deforested region of the Brazilian Amazon basin. *Biogeochemistry* **68**:227-257.
- Boyer, E. W., R. B. Alexander, W. J. Parton, C. S. Li, K. Butterbach-Bahl, S. D. Donner, R. W. Skaggs, and S. J. Del Gross. 2006. Modeling denitrification in terrestrial and aquatic ecosystems at regional scales. *Ecological Applications* **16**:2123-2142.
- Butturini, A. and F. Sabater. 1998. Ammonium and phosphate retention in a Mediterranean stream: hydrological versus temperature control. *Canadian Journal of Fisheries and Aquatic Sciences* **55**:1938-1945.
- Claessens, L. and C. L. Tague. 2009. Transport-based method for estimating in-stream nitrogen uptake at ambient concentration from nutrient addition experiments. *Limnology and Oceanography-Methods* **7**:811-822.
- Claessens, L., C. L. Tague, L. E. Band, P. M. Groffman, and S. T. Kenworthy. 2009. Hydro-ecological linkages in urbanizing watersheds: An empirical assessment of in-stream nitrate loss and evidence of saturation kinetics. *Journal of Geophysical Research-Biogeosciences* **114**:12.
- Covino, T. P. and B. L. McGlynn. 2007. Stream gains and losses across a mountain to valley transition: Impacts on watershed hydrology and stream water chemistry. *Water Resources Research* **43**, W10431, doi:10.1029/2006WR005544.
- Covino, T. P., B. L. McGlynn, and M. A. Baker. 2010. Separating physical and biological nutrient retention and quantifying uptake kinetics from ambient to saturation in successive mountain stream reaches *Journal of Geophysical Research - Biogeosciences*.

- Covino, T. P., B. L. McGlynn, and R. A. McNamara. in press. Quantifying stream nutrient uptake kinetics from ambient to saturation: Tracer Additions for Spiraling Curve Characterization. *Limnology and Oceanography: Methods*.
- Creed, I. F. and L. E. Band. 1998. Exploring functional similarity in the export of nitrate-N from forested catchments: A mechanistic modeling approach. *Water Resources Research* **34**:3079-3093.
- Davis, J. C. and G. W. Minshall. 1999. Nitrogen and phosphorus uptake in two Idaho (USA) headwater wilderness streams. *Oecologia* **119**:247-255.
- Day, T. J. 1976. Precision of salt dilution gauging. *Journal of Hydrology* **31**:293-306.
- Dingman, S. L. 2002. Stream-gauging methods for short-term studies. *in* S. L. Dingman, editor. *Physical Hydrology*. Prentice Hall, Upper Saddle River.
- Dodds, W. K., A. J. Lopez, W. B. Bowden, S. Gregory, N. B. Grimm, S. K. Hamilton, A. E. Hershey, E. Marti, W. H. McDowell, J. L. Meyer, D. Morrall, P. J. Mulholland, B. J. Peterson, J. L. Tank, H. M. Valett, J. R. Webster, and W. Wollheim. 2002. N uptake as a function of concentration in streams. *Journal of the North American Benthological Society* **21**:206-220.
- Dugdale, R. C. 1967. Nutrient Limitation in sea - dynamics identification and significance. *Limnology and Oceanography* **12**:685-&.
- Earl, S. R., H. M. Valett, and J. R. Webster. 2006. Nitrogen saturation in stream ecosystems. *Ecology* **87**:3140-3151.
- Elser, J. J., M. E. S. Bracken, E. E. Cleland, D. S. Gruner, W. S. Harpole, H. Hillebrand, J. T. Ngai, E. W. Seabloom, J. B. Shurin, and J. E. Smith. 2007. Global analysis of nitrogen and phosphorus limitation of primary producers in freshwater, marine and terrestrial ecosystems. *Ecology Letters* **10**:1135-1142.
- Ensign, S. H. and M. W. Doyle. 2006. Nutrient spiraling in streams and river networks. *Journal of Geophysical Research-Biogeosciences* **111**:13.
- Gardner, K. K. and B. L. McGlynn. 2009. Seasonality in spatial variability and influence of land use/land cover and watershed characteristics on streamwater nitrate concentrations in a developing watershed in the Rocky Mountain West. *Water Resources Research* **45**.
- Hall, R. O., E. S. Bernhardt, and G. E. Likens. 2002. Relating nutrient uptake with transient storage in forested mountain streams. *Limnology and Oceanography* **47**:255-265.

- Hall, R. O., J. L. Tank, D. J. Sobota, P. J. Mulholland, J. M. O'Brien, W. K. Dodds, J. R. Webster, H. M. Valett, G. C. Poole, B. J. Peterson, J. L. Meyer, W. H. McDowell, S. L. Johnson, S. K. Hamilton, N. B. Grimm, S. V. Gregory, C. N. Dahm, L. W. Cooper, L. R. Ashkenas, S. M. Thomas, R. W. Sheibley, J. D. Potter, B. R. Niederlehner, L. T. Johnson, A. M. Helton, C. M. Crenshaw, A. J. Burgin, M. J. Bernot, J. J. Beaulieu, and C. P. Arango. 2009. Nitrate removal in stream ecosystems measured by N-15 addition experiments: Total uptake. *Limnology and Oceanography* **54**:653-665.
- Hart, B. T., P. Freeman, and I. D. McKelvie. 1992. Whole-stream phosphorus release studies - variation in uptake length with initial phosphorus concentration. *Hydrobiologia* **235**:573-584.
- Kaushal, S. S., W. M. Lewis, and J. H. McCutchan. 2006. Land use change and nitrogen enrichment of a Rocky Mountain watershed. *Ecological Applications* **16**:299-312.
- Kennedy, C. D., D. P. Genereux, D. R. Corbett, and H. Mitasova. 2009. Spatial and temporal dynamics of coupled groundwater and nitrogen fluxes through a streambed in an agricultural watershed. *Water Resources Research* **45**:18.
- Kilpatrick, F. A. and E. D. Cobb. 1985. Measurement of discharge using tracers. U.S. Geological Survey, *Techniques of Water-Resources Investigations*, Book 3, Chapter A16.
- Marti, E. and F. Sabater. 1996. High variability in temporal and spatial nutrient retention in Mediterranean streams. *Ecology* **77**:854-869.
- Mueller, D. K. and N. E. Spahr. 2006. Nutrients in Streams and Rivers Across the Nation — 1992–2001. Page 51 in USGS, editor.
- Mulholland, P. J., A. M. Helton, G. C. Poole, R. O. Hall, S. K. Hamilton, B. J. Peterson, J. L. Tank, L. R. Ashkenas, L. W. Cooper, C. N. Dahm, W. K. Dodds, S. E. G. Findlay, S. V. Gregory, N. B. Grimm, S. L. Johnson, W. H. McDowell, J. L. Meyer, H. M. Valett, J. R. Webster, C. P. Arango, J. J. Beaulieu, M. J. Bernot, A. J. Burgin, C. L. Crenshaw, L. T. Johnson, B. R. Niederlehner, J. M. O'Brien, J. D. Potter, R. W. Sheibley, D. J. Sobota, and S. M. Thomas. 2008. Stream denitrification across biomes and its response to anthropogenic nitrate loading. *Nature* **452**:202-U246.
- Mulholland, P. J., J. D. Newbold, J. W. Elwood, L. A. Ferren, and J. R. Webster. 1985. Phosphorus spiraling in a woodland stream - seasonal-variations. *Ecology* **66**:1012-1023.

- Mulholland, P. J., J. L. Tank, J. R. Webster, W. B. Bowden, W. K. Dodds, S. V. Gregory, N. B. Grimm, S. K. Hamilton, S. L. Johnson, E. Marti, W. H. McDowell, J. L. Merriam, J. L. Meyer, B. J. Peterson, H. M. Valett, and W. M. Wollheim. 2002. Can uptake length in streams be determined by nutrient addition experiments? Results from an interbiome comparison study. *Journal of the North American Benthological Society* **21**:544-560.
- Mulholland, P. J. and J. R. Webster. 2010. Nutrient dynamics in streams and the role of J-NABS. *Journal of the North American Benthological Society* **29**:100-117.
- National Science Foundation. 1976. Impacts of large recreational development upon semi-primitive environments, final report. Arlington, VA.
- Newbold, J. D., T. L. Bott, L. A. Kaplan, C. L. Dow, J. K. Jackson, A. K. Aufdenkampe, L. A. Martin, D. J. Van Horn, and A. A. de Long. 2006. Uptake of nutrients and organic C in streams in New York City drinking-water-supply watersheds. *Journal of the North American Benthological Society* **25**:998-1017.
- Newbold, J. D., J. W. Elwood, R. V. Oneill, and W. Vanwinkle. 1981. Measuring nutrient spiralling in streams. *Canadian Journal of Fisheries and Aquatic Sciences* **38**:860-863.
- O'Brien, J. M., W. K. Dodds, K. C. Wilson, J. N. Murdock, and J. Eichmiller. 2007. The saturation of N cycling in Central Plains streams: N-15 experiments across a broad gradient of nitrate concentrations. *Biogeochemistry* **84**:31-49.
- Payn, R. A., M. N. Gooseff, B. L. McGlynn, K. E. Bencala, and S. M. Wondzell. 2009. Channel water balance and exchange with subsurface flow along a mountain headwater stream in Montana, United States. *Water Resour. Res.* **45**.
- Payn, R. A., J. R. Webster, P. J. Mulholland, H. M. Valett, and W. K. Dodds. 2005. Estimation of stream nutrient uptake from nutrient addition experiments. *Limnology and Oceanography-Methods* **3**:174-182.
- Peterson, B. J., W. M. Wollheim, P. J. Mulholland, J. R. Webster, J. L. Meyer, J. L. Tank, E. Marti, W. B. Bowden, H. M. Valett, A. E. Hershey, W. H. McDowell, W. K. Dodds, S. K. Hamilton, S. Gregory, and D. D. Morrall. 2001. Control of nitrogen export from watersheds by headwater streams. *Science* **292**:86-90.
- Rabalais, N. N., R. J. Diaz, L. A. Levin, R. E. Turner, D. Gilbert, and J. Zhang. 2010. Dynamics and distribution of natural and human-caused hypoxia. *Biogeosciences* **7**:585-619.

- Royer, T. V., J. L. Tank, and M. B. David. 2004. Transport and fate of nitrate in headwater agricultural streams in Illinois. *Journal of Environmental Quality* **33**:1296-1304.
- Ruggiero, A., A. G. Solimini, M. Anello, A. Romano, M. De Cicco, and G. Carchini. 2006. Nitrogen and phosphorus retention in a human altered stream. *Chemistry and Ecology* **22**:1-13.
- Sanderson, B. L., H. J. Coe, C. D. Tran, K. H. Macneale, D. L. Harstad, and A. B. Goodwin. 2009. Nutrient limitation of periphyton in Idaho streams: results from nutrient diffusing substrate experiments. *Journal of the North American Benthological Society* **28**:832-845.
- Sickman, J. O. and J. M. Melack. 1998. Nitrogen and sulfate export from high elevation catchments of the Sierra Nevada, California. *Water Air and Soil Pollution* **105**:217-226.
- Simon, K. S., C. R. Townsend, B. J. F. Biggs, and W. B. Bowden. 2005. Temporal variation of N and P uptake in 2 New Zealand streams. *Journal of the North American Benthological Society* **24**:1-18.
- Stream Solute Workshop. 1990. Concepts and Methods for Assessing Solute Dynamics in Stream Ecosystems. *Journal of the North American Benthological Society* **9**:95-119.
- Tank, J. L., E. J. Rosi-Marshall, M. A. Baker, and R. O. Hall. 2008. Are rivers just big streams? A pulse method to quantify nitrogen demand in a large river. *Ecology* **89**:2935-2945.
- Triska, F. J., V. C. Kennedy, R. J. Avanzino, G. W. Zellweger, and K. E. Bencala. 1989a. Retention and transport of nutrients in a 3rd-order stream - channel processes. *Ecology* **70**:1877-1892.
- Triska, F. J., V. C. Kennedy, R. J. Avanzino, G. W. Zellweger, and K. E. Bencala. 1989b. Retention and transport of nutrients in a 3rd-order stream in Northwestern California - hyporheic processes. *Ecology* **70**:1893-1905.
- U.S. Department of Agriculture, F. S. 1994. Ecoregions of the United States: <http://www.fs.fed.us/land/pubs/ecoregions/>.
- Valett, H. M., J. A. Morrice, C. N. Dahm, and M. E. Campana. 1996. Parent lithology, surface-groundwater exchange, and nitrate retention in headwater streams. *Limnology and Oceanography* **41**:333-345.

- Webster, J. R. and B. C. Patten. 1979. EFFECTS OF WATERSHED PERTURBATION ON STREAM POTASSIUM AND CALCIUM DYNAMICS. *Ecological Monographs* **49**:51-72.
- Webster, J. R. and H. M. Valett. 2006. Solute Dynamics. Pages 169-185 *in* F. R. Hauer and G. A. Lamberti, editors. *Methods in Stream Ecology*. Elsevier, Burlington, MA. .
- Whitehead, P. G., P. J. Johnes, and D. Butterfield. 2002. Steady state and dynamic modelling of nitrogen in the River Kennet: impacts of land use change since the 1930s. *Science of the Total Environment* **282**:417-434.
- Williams, M. W., J. S. Baron, N. Caine, R. Sommerfeld, and R. Sanford. 1996. Nitrogen saturation in the Rocky Mountains. *Environmental Science & Technology* **30**:640-646.
- Wollheim, W. M., B. J. Peterson, S. M. Thomas, C. H. Hopkinson, and C. J. Vorosmarty. 2008. Dynamics of N removal over annual time periods in a suburban river network. *Journal of Geophysical Research-Biogeosciences* **113**:17.
- Wondzell, S. M., M. N. Gooseff, and B. L. McGlynn. 2007. Flow velocity and the hydrologic behavior of streams during baseflow. *Geophysical Research Letters* **34**.

Table 1: Location, reach characteristics and season of tracer addition experiments conducted in the West Fork Gallatin Watershed

| Streams | Discharge ¹ ($\text{m}^3 \text{s}^{-1}$) | Watershed area (km^2) | Ambient nitrate levels ($\text{NO}_3\text{-N } \mu\text{g L}^{-1}$) | Season of experiments ² |
|----------------------|--|-------------------------------------|--|---------------------------------------|
| Beehive | Low (< 0.14) | Small (< 10) | Low (< 15) ³ | Summer, Fall, and Winter |
| Pony | Low (< 0.14) | Small (< 10) | High (≥ 15) | Summer |
| Upper Middle Fork | Medium (0.14 – 0.20) | Medium (10 – 50) | High (≥ 15) | Summer |
| North Fork | Medium (0.14 – 0.20) | Medium (10 – 50) | Low (< 15) | Summer |
| Lower Middle Fork | High (> 0.20) | Large (> 50) | High (≥ 15) | Summer |
| West Fork | High (> 0.20) | Large (> 50) | Low (< 15) | Summer |

¹Summer baseline discharge levels

²Summer experiments were conducted between June 1 and September 15; Fall experiments were conducted between October 1 and November 15; Winter experiments were conducted in March.

³The Beehive March 2009 ambient $\text{NO}_3\text{-N}$ level was > 15 $\mu\text{g L}^{-1}$

Table 2: Dates when tracer addition experiments were conducted, physical characteristics, ambient NO₃-N concentrations for the day of the experiment and average annual NO₃-N concentrations for the six experimental stream reaches, note that multiple tracer addition experiments were conducted at Beehive to explore seasonal effects.

| Site | Date | Experiment Method | Watershed area (km ²) | Slope of experimental reach (%) | Stream Order | Downstream Q (m ³ s ⁻¹) | Median Flow Velocity (m s ⁻¹) | Distance (m) | Stream temperature (°C) | Ambient [NO ₃ -N] (µg l ⁻¹) | Average annual [NO ₃ -N] (µg l ⁻¹) |
|-------------------|---------------|-------------------|-----------------------------------|---------------------------------|--------------|--|---|--------------|-------------------------|--|---|
| | Aug-07 | | | | | | | | | | |
| Pony | 24-Aug-07 | Slug | 0.90 | 8.8 | 1 | 0.006 | 0.099 | 625 | 4.77-8.74 | 68.3 | 202 |
| | Jul-08 | | | | | | | | | | |
| Beehive | 29-Jul-08 | Slug | 5.7 | 1.7 | 2 | 0.137 | 0.342 | 588 | 7.9-12.4 | 2.00 | 20.8 |
| | 30-Jul-08 | Plat. | 5.7 | 1.7 | 2 | 0.121 | 0.329 | 588 | 7.0-10.9 | 2.00 | 20.8 |
| | 30-Jul-08 | Plat. | 5.7 | 1.7 | 2 | 0.121 | 0.329 | 588 | 7.0-10.9 | 2.00 | 20.8 |
| | Oct-06 | | | | | | | | | | |
| Beehive | 13-Oct-06 | Slug | 5.7 | 1.7 | 2 | 0.027 | 0.117 | 545 | N/A | 1.83 | 20.8 |
| | Mar-07 | | | | | | | | | | |
| Beehive | 25-Mar-07 | Slug | 5.7 | 1.7 | 2 | 0.009 | 0.080 | 523 | 0.152-1.96 | 10.5 | 20.8 |
| | Oct-07 | | | | | | | | | | |
| Beehive | 31-Oct-07 | Slug | 5.7 | 1.7 | 2 | 0.018 | 0.154 | 575 | -0.237-0.205 | 4.42 | 20.8 |
| | Mar-09 | | | | | | | | | | |
| Beehive | 16-Mar-09 | Slug | 5.7 | 1.7 | 2 | 0.003 | 0.041 | 545 | -0.075-0.13 | 89.7 | 20.8 |
| | Jul-07 | | | | | | | | | | |
| North Fork | 25-Jul-07 | "Slug" for Plat. | 22.8 | 8.6 | 2 | 0.162 | 0.248 | 1050 | 8.72-12.3 | 5.74 | 38.4 |
| | 26-Jul-07 | "Slug" for Plat. | 22.8 | 8.6 | 2 | 0.146 | 0.253 | 1050 | 8.77-12.5 | 5.74 | 38.4 |
| | Aug-07 | | | | | | | | | | |
| Upper Middle Fork | 1-Aug-07 | "Slug" for Plat. | 28.3 | 3.7 | 2 | 0.148 | 0.244 | 1043 | 10.1-18.4 | 16.8 | 91.6 |
| | 2-Aug-07 | "Slug" for Plat. | 28.3 | 3.7 | 2 | 0.142 | 0.240 | 1043 | 10.7-17.3 | 16.8 | 91.6 |
| | Aug-07 | | | | | | | | | | |
| Lower Middle Fork | 21-Aug-07 | Slug | 83.4 | 1.0 | 3 | 0.311 | 0.219 | 1286 | 12.3-16.7 | 43.6 | 213 |
| | 23-Aug-07 | Slug | 83.4 | 1.0 | 3 | 0.218 | 0.205 | 1286 | 9.2-13.8 | 43.6 | 213 |
| | 22-Aug-07 | Plat. | 83.4 | 1.0 | 3 | 0.245 | 0.210 | 1286 | 11.0-15.3 | 43.6 | 213 |
| | Jul-08 | | | | | | | | | | |
| West Fork | 25-Jul-08 | Slug | 240 | 1.1 | 4 | 2.47 | 0.768 | 1075 | 8.12-15.3 | 3.96 | 132 |
| | 25-Jul-08 | Slug | 240 | 1.1 | 4 | 2.44 | 0.762 | 1075 | 8.12-15.3 | 3.96 | 132 |

For Experimental Methods column:

Slug is when an instantaneous tracer addition experiment was performed

Plat. is when a constant-rate tracer addition experiment was performed

"Slug" for Plat. is when a constant-rate tracer addition experiment was conducted and the data from the rising and falling limbs to and from SC plateau were analyzed with the same method as an instantaneous tracer addition experiment

Table 3: Total, physical, and biological NO₃-N retention for each instantaneous tracer addition. Total NO₃-N retention is the amount of NO₃-N added at the upstream endpoint of the experimental stream reach that is not measured at the downstream endpoint; it is the sum of physical and biological NO₃-N retention. Physical NO₃-N retention is hydrologic retention (e.g. water moving into the groundwater, hyporheic zones, etc.) that does not return to the experimental stream reach in the duration of the experiment. Biological NO₃-N retention is the NO₃-N retained from the water column through biological processes (e.g., NO₃-N uptake).

| Site | Date | Experiment Method | Ambient [NO ₃ -N] (µg l ⁻¹) | Total NO ₃ -N Retention (%) | Physical NO ₃ -N Retention (%) | Biological NO ₃ -N Retention (%) | Biological: Total NO ₃ -N Retention (%) |
|-------------------|---------------|-----------------------------|---|---|--|--|---|
| | Aug-07 | | | | | | |
| Pony | 24-Aug-07 | Slug | 68.3 | 86.7 | 81.2 | 5.5 | 6.4 |
| | Jul-08 | | | | | | |
| Beehive | 29-Jul-08 | Slug | 2.00 | 53.3 | 42.2 | 11.1 | 20.9 |
| | 30-Jul-08 | Plat. | 2.00 | | | | |
| | 30-Jul-08 | Plat. | 2.00 | | | | |
| | Oct-06 | | | | | | |
| Beehive | 13-Oct-06 | Slug | 1.83 | 86.9 | 85.4 | 1.5 | 1.7 |
| | Mar-07 | | | | | | |
| Beehive | 25-Mar-07 | Slug | 10.5 | 92.2 | 88.1 | 4.1 | 4.5 |
| | Oct-07 | | | | | | |
| Beehive | 31-Oct-07 | Slug | 4.42 | 72.1 | 64.5 | 7.7 | 10.6 |
| | Mar-09 | | | | | | |
| Beehive | 16-Mar-09 | Slug | 89.7 | 90.9 | 89.1 | 1.8 | 2.0 |
| | Jul-07 | | | | | | |
| North Fork | 25-Jul-07 | "Slug" for Plat. | 5.74 | 83.7 | 72.2 | 11.5 | 13.7 |
| | 26-Jul-07 | "Slug" for Plat. | 5.74 | 69.6 | 55.0 | 14.6 | 21.0 |
| | | Comb. "Slug" for both Plat. | 5.74 | 76.6 | 63.6 | 13.0 | 17.0 |
| | Aug-07 | | | | | | |
| Upper Middle Fork | 1-Aug-07 | "Slug" for Plat. | 16.8 | -6.9 | -94.4 | 87.6 | -1278.3 |
| | 2-Aug-07 | "Slug" for Plat. | 16.8 | 23.7 | -53.3 | 76.4 | 330.8 |
| | | Comb. "Slug" for both Plat. | 17.8 | 8.1 | -73.9 | 82.0 | 1009.3 |
| | Aug-07 | | | | | | |
| Lower Middle Fork | 21-Aug-07 | Slug | 43.6 | 78.8 | 33.3 | 45.5 | 57.7 |
| | 23-Aug-07 | Slug | 43.6 | 50.2 | 13.4 | 36.8 | 73.3 |
| | 22-Aug-07 | "Slug" for Plat. | 43.6 | 60.3 | 26.3 | 33.9 | 56.3 |
| | | Comb. Slugs and Plat. | 43.6 | 63.1 | 24.4 | 38.7 | 61.4 |
| | Jul-08 | | | | | | |
| West Fork | 25-Jul-08 | Slug | 3.96 | 65.3 | 9.1 | 56.3 | 86.1 |
| | 25-Jul-08 | Slug | 3.96 | 64.6 | 7.5 | 57.1 | 88.3 |
| | | Comb. Slugs | 3.96 | 65.0 | 8.3 | 56.7 | 87.2 |

For Experimental Methods column:

Slug is when an instantaneous tracer addition experiment was performed

Plat. is when a constant-rate tracer addition experiment was performed

"Slug" for Plat. is when a constant-rate tracer addition experiment was conducted and the data from the rising and falling limbs to and from SC plateau were analyzed with the same method as an instantaneous tracer addition experiment

"Slug" for both Plat. is when two constant-rate tracer addition experiments were conducted and the data from the rising and falling limbs of both plateau experiments were analyzed with the same method as an instantaneous addition experiment

Comb. written before any of the terms means the data from the said experiments were combined

Italicized numbers were not used in figures or comparisons

Bolded numbers were the set of values used in figures when there were more than one set of values for one stream experimental reach

Table 4: Ambient uptake parameters including ambient uptake length (S_{w-amb}), ambient uptake velocity (V_{f-amb}), ambient areal uptake rate (U_{amb}), and Michaelis-Menten (M-M) uptake parameters (U_{max} and K_m) for each tracer addition experiment.

| Site | Date | Experiment Method | Ambient [NO ₃ -N] (µg l ⁻¹) | Total [NO ₃ -N] (µg l ⁻¹) | Mass Added [NO ₃ -N] (g) | S_{w-amb} (m) | V_{f-amb} (mm min ⁻¹) | U_{amb} (µg m ⁻² min ⁻¹) | P-value for S_{w-amb} ($\alpha = 0.05$) | U_{max} (µg m ⁻² min ⁻¹) | K_m (µg l ⁻¹) | r^2 for M-M model fits | p-value for M-M model fits |
|-------------------|-----------|---|---|---|--|--------------------|--|--|--|--|--------------------------------|-----------------------------|-------------------------------|
| Pony | Aug-07 | Slug | 68.3 | 481 | 34.6 | 625 | 0.823 | 56.2 | 0.0027 | 357 | 508 | 0.88 | <0.0001 |
| | 24-Aug-07 | | | | | | | | | | | | |
| | Jul-08 | | | | | | | | | | | | |
| Beehive | 29-Jul-08 | Slug Plat. Plat. | 2.00 | 47.4 | 13.9 | 1171 | 4.99 | 9.99 | 0.0003 | 197 | 23 | 0.71 | 0.0001 |
| | 30-Jul-08 | | | | | | | | | | | | |
| | 30-Jul-08 | | | | | | | | | | | | |
| Beehive | 13-Oct-06 | Slug | 1.83 | 101 | 38.1 | 171 | 7.80 | 14.2 | 0.0069 | 49 | 7.4 | 0.56 | 0.0521 |
| | Mar-07 | | | | | | | | | | | | |
| | 25-Mar-07 | | | | | | | | | | | | |
| Beehive | 31-Oct-07 | Slug | 10.5 | 25.3 | 1.4 | -1938 | -0.299 | -3.13 | 0.0589 | 3.8 | 5.9 | 0.02 | 0.8218 |
| | Mar-09 | | | | | | | | | | | | |
| | 16-Mar-09 | | | | | | | | | | | | |
| North Fork | 25-Jul-07 | "Slug" for Plat. "Slug" for Plat. Comb. "Slug" for both Plat. | 5.74 | 42.1 | 208 | 1099 | 5.42 | 31.1 | 0.0173 | | | | |
| | 26-Jul-07 | | | | | | | | | | | | |
| | Aug-07 | | | | | | | | | | | | |
| Upper Middle Fork | 1-Aug-07 | "Slug" for Plat. "Slug" for Plat. Comb. "Slug" for both Plat. | 16.8 | 228 | 202 | 1146 | 4.09 | 68.5 | 0.0289 | | | | |
| | 2-Aug-07 | | | | | | | | | | | | |
| | Aug-07 | | | | | | | | | | | | |
| Lower Middle Fork | 21-Aug-07 | Slug Plat. Comb. Slugs | 43.6 | 53.6 | 24.5 | -461 | -9.42 | -411 | 0.0002 | | | | |
| | 23-Aug-07 | | | | | | | | | | | | |
| | 22-Aug-07 | | | | | | | | | | | | |
| West Fork | 25-Jul-08 | Slug Slug Comb. Slugs | 3.96 | 9.1 | 27.7 | 881 | 42.0 | 166 | 0.1030 | | | | |
| | 25-Jul-08 | | | | | | | | | | | | |
| | Aug-07 | | | | | | | | | | | | |

For Experimental Methods column:

Slug is when an instantaneous tracer addition experiment was performed

Plat. is when a constant-rate tracer addition experiment was performed

"Slug" for Plat. is when a constant-rate tracer addition experiment was conducted and the data from the rising and falling limbs to and from SC plateau

were analyzed with the same method as an instantaneous tracer addition experiment

"Slug" for both Plat. is when two constant-rate tracer addition experiments were conducted and the data from the rising and falling limbs of both plateau

experiments were analyzed with the same method as an instantaneous addition experiment

Comb. written before any of the terms indicates the data from the said experiments were combined

Numbers that are **bold** and in *italics* are numbers with p-values < α (values that were not significant)

Exception: Lower Middle Fork August 21, 2007, the y-intercept was negative

Table 5: Uptake dynamics for constant-rate tracer addition experiments. Two additions were conducted at Beehive: a low and high $[\text{NO}_3\text{-N}]_{\text{tot-plat}}$ addition. $[\text{NO}_3\text{-N}]_{\text{tot-plat}}$ is the geometric mean of total $\text{NO}_3\text{-N}$ concentrations (non-background corrected) for the longitudinal stream samples collected along the stream reach during the specific conductance plateau of the constant-rate addition. $S_{w\text{-add-plat}}$ is the uptake length of added nutrient, $V_{f\text{-tot-plat}}$ is total nutrient uptake velocity, and $U_{\text{tot-plat}}$ is the total areal uptake rate each calculated using the plateau approach.

| Site | Date | $[\text{NO}_3\text{-N}_{\text{amb}}]$ ($\mu\text{g l}^{-1}$) | $[\text{NO}_3\text{-N}_{\text{tot-plat}}]$ ($\mu\text{g l}^{-1}$) | $S_{w\text{-add-plat}}$ (m) | $V_{f\text{-tot-plat}}$ (mm min^{-1}) | $U_{\text{tot-plat}}$ ($\mu\text{g m}^{-2} \text{min}^{-1}$) | P-value for $S_{w\text{-add-plat}}$ |
|-------------------|-----------|---|--|--------------------------------|---|---|--|
| Jul-08 | | | | | | | |
| Beehive | 30-Jul-08 | 2.00 | 23 | 2534 | 2.38 | 54 | 0.1474 |
| | 30-Jul-08 | 2.00 | 103 | 4140 | 1.37 | 141 | <0.0001 |
| Aug-07 | | | | | | | |
| Lower Middle Fork | 22-Aug-07 | 43.6 | 516 | 3484 | 1.53 | 788 | 0.0997 |

The numbers that are **bold** and in *italics* have $p\text{-values} > \alpha$ (values that were not significant)

Table 6: Breakthrough curve (BTC) integrated uptake dynamics for instantaneous tracer addition experiments. $[\text{NO}_3\text{-N}_{\text{tot-int}}]$ is the geometric mean of non-background corrected total observed and conservative $\text{NO}_3\text{-N}$ BTC-integrated concentrations. $S_{w\text{-add-int}}$ is the uptake length of added nutrient, $V_{f\text{-tot-int}}$ is total nutrient uptake velocity, and $U_{\text{tot-int}}$ is the total areal uptake rate of added nutrient each calculated through BTC-integration.

| Site | Date | $[\text{NO}_3\text{-N}_{\text{amb}}]$ ($\mu\text{g l}^{-1}$) | $[\text{NO}_3\text{-N}_{\text{tot-int}}]$ ($\mu\text{g l}^{-1}$) | $S_{w\text{-add-int}}$ (m) | $V_{f\text{-tot-int}}$ (mm min^{-1}) | $U_{\text{tot-int}}$ ($\mu\text{g m}^{-2} \text{min}^{-1}$) |
|-------------------|---------------|---|---|-------------------------------|--|--|
| | Aug-07 | | | | | |
| Pony | 24-Aug-07 | 68.3 | 481 | 1804 | 0.349 | 168 |
| | Jul-08 | | | | | |
| Beehive | 29-Jul-08 | 2.0 | 47 | 2753 | 2.31 | 110 |
| | Oct-06 | | | | | |
| Beehive | 13-Oct-06 | 1.83 | 101 | 5081 | 0.400 | 40.2 |
| | Mar-07 | | | | | |
| Beehive | 25-Mar-07 | 10.5 | 25 | 1225 | 0.154 | 3.90 |
| | Oct-07 | | | | | |
| Beehive | 31-Oct-07 | 4.42 | 95 | 2373 | 0.542 | 51.5 |
| | Mar-09 | | | | | |
| Beehive | 16-Mar-09 | 89.7 | 522 | 2961 | 0.070 | 36.5 |
| | Jul-07 | | | | | |
| North Fork | 25-Jul-07 | 5.74 | 42 | 1972 | 3.24 | 137 |
| | 26-Jul-07 | 5.74 | 65 | 2683 | 2.37 | 154 |
| | Aug-07 | | | | | |
| Upper Middle Fork | 1-Aug-07 | 16.8 | 228 | 1742 | 2.82 | 642 |
| | 2-Aug-07 | 16.8 | 377 | 1512 | 3.02 | 1140 |
| | Aug-07 | | | | | |
| Lower Middle Fork | 21-Aug-07 | 43.6 | 54 | 1120 | 4.60 | 247 |
| | 23-Aug-07 | 43.6 | 214 | 2323 | 2.44 | 523 |
| | Jul-08 | | | | | |
| West Fork | 25-Jul-08 | 3.96 | 9 | 1115 | 44.2 | 405 |
| | 25-Jul-08 | 3.96 | 124 | 1120 | 33.5 | 4155 |

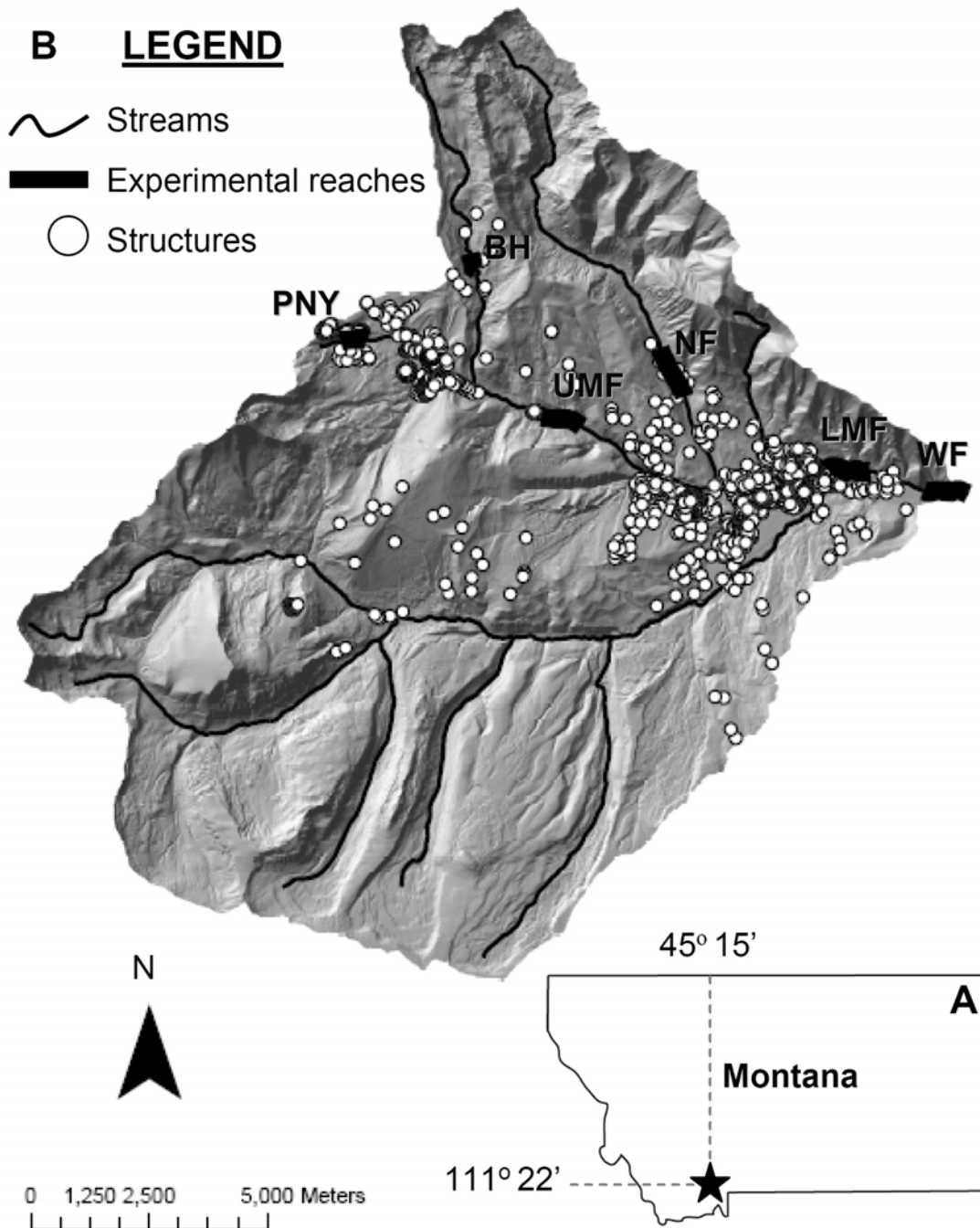


Figure 2.1: (A) Map of Montana showing the location of the West Fork Gallatin Watershed, and (B) shows location of each of the six experimental stream reach within the watershed. The dots on the map represent structure locations. Abbreviated names are next to each experimental stream reach; BH is Beehive, PNY is Pony, UMF is Upper Middle Fork, NF is North Fork, LMF is Lower Middle Fork, and WF is West Fork

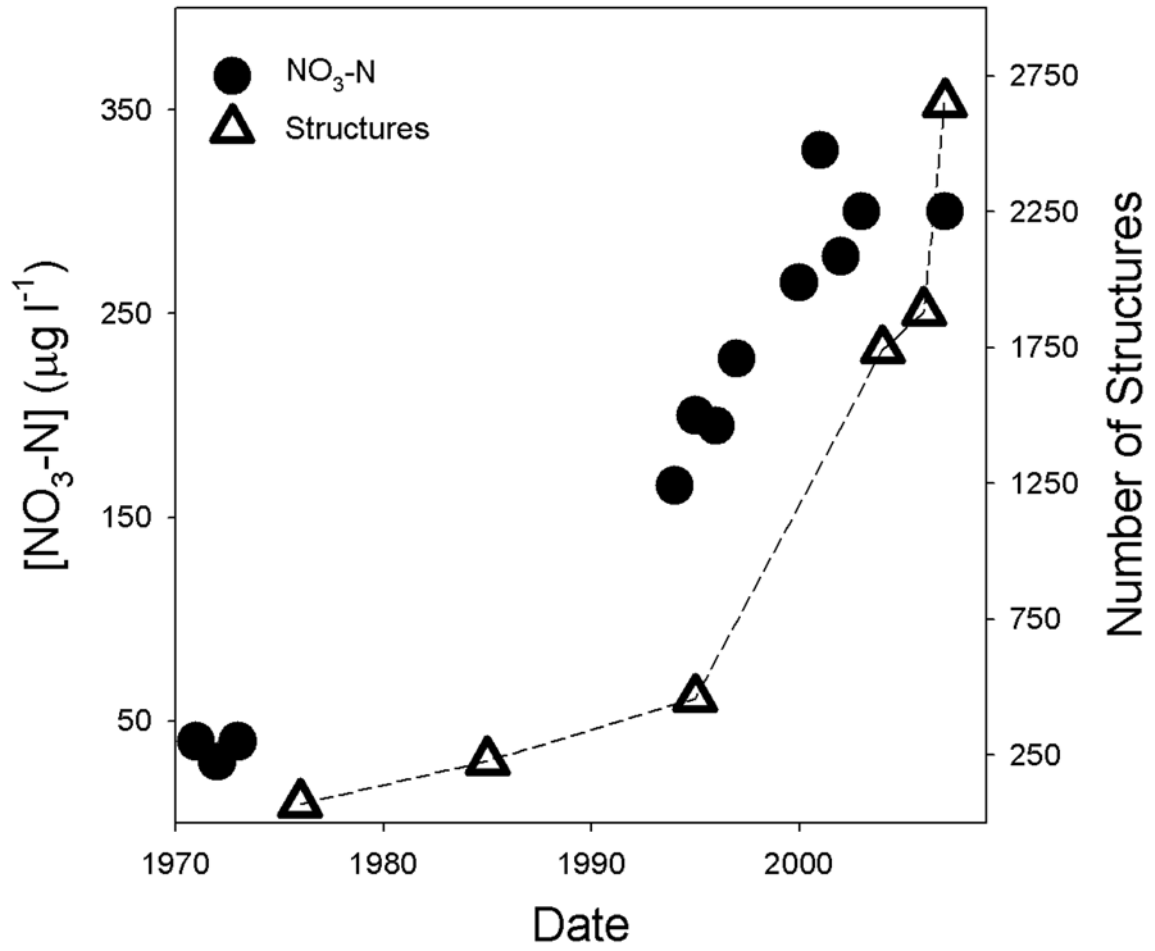


Figure 2.2: Time series of the number of structures and average annual ambient NO₃-N concentrations over the last forty years in the West Fork Gallatin Watershed.

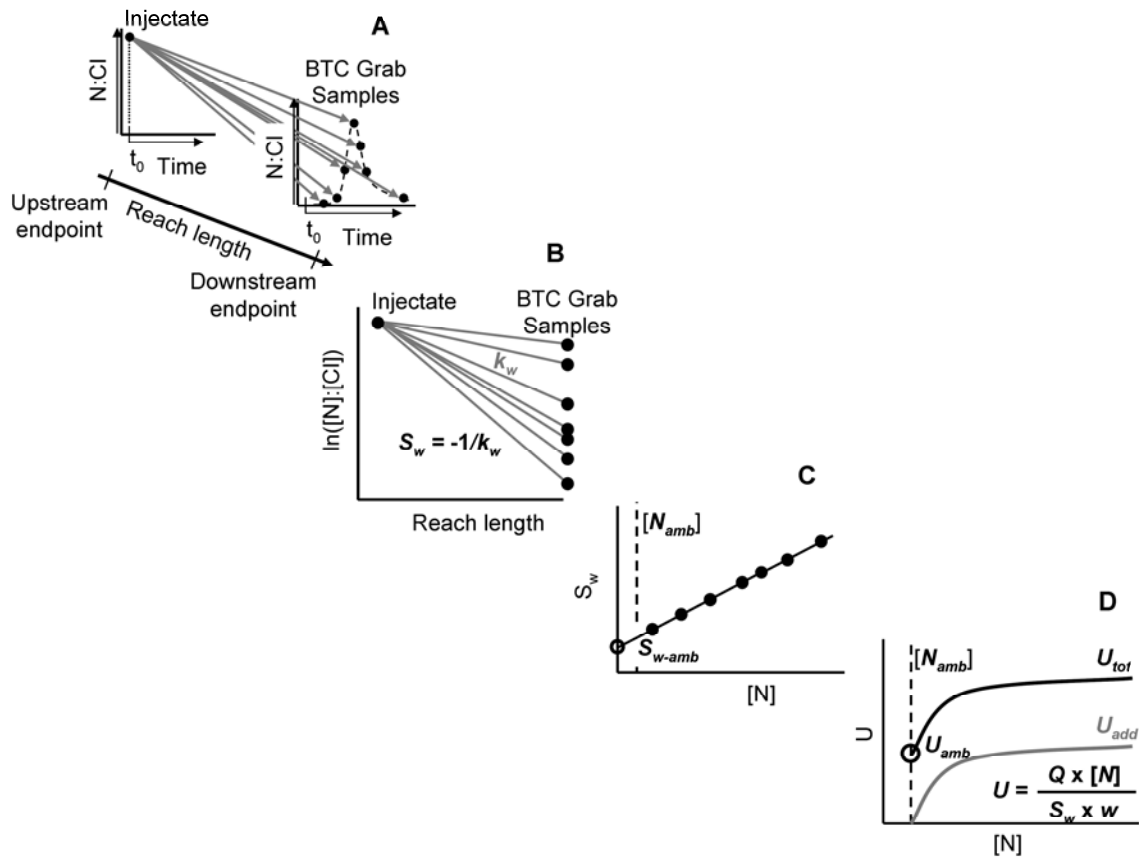


Figure 2.3: Conceptual model describing calculations of uptake length (S_w) and areal uptake rate (U) from NO_3 -N and Cl concentrations measured during the experimental breakthrough curve (BTC). (A) The NO_3 -N:Cl was measured for the injectate and for each grab sample taken during the BTC. (B) The slope of the linear regression between the natural log of NO_3 -N:Cl of the injectate sample and each of the BTC grab samples yields the uptake rate for each sample (k_w). (C) The y-intercept of the linear regression through each of the calculated S_w values yields the ambient uptake length (S_{w-amb}). (D) U values are calculated from S_w values. For each grab sample, ambient areal uptake rate (U_{amb}) is added to each areal uptake rate of added nutrient (U_{add}) to calculate the total areal uptake rate (U_{tot}).

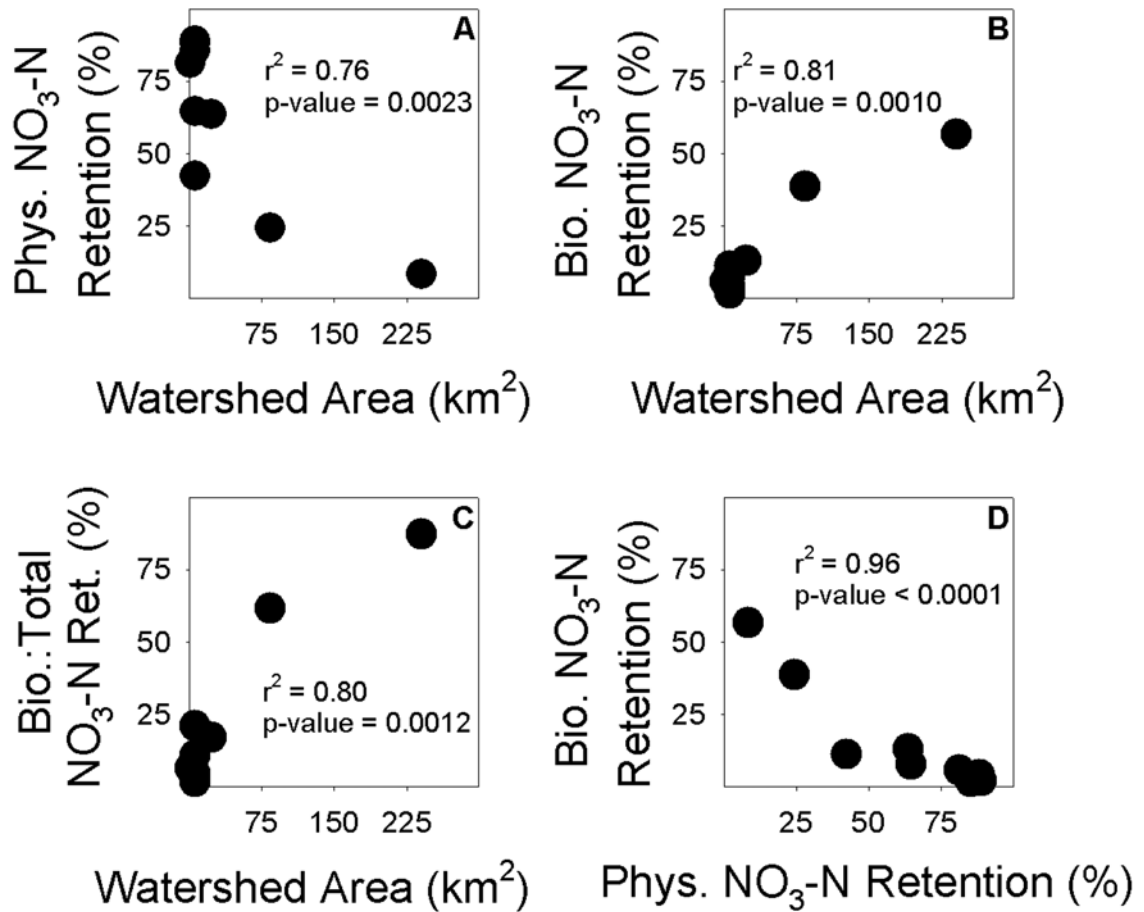


Figure 2.4: (A) Physical and (B) biological NO₃-N retention for five of six stream reaches versus their watershed areas. NO₃-N retention values for the Upper Middle Fork were inconsistent with the other five experimental stream reaches and therefore not included in this figure. (C) The ratio of biologic to total NO₃-N retention versus watershed area. (D) Biologic NO₃-N retention versus physical NO₃-N retention. (A) and (D) both demonstrate significant exponential decay relationships and (B) and (C) have significant logarithmic relationships.

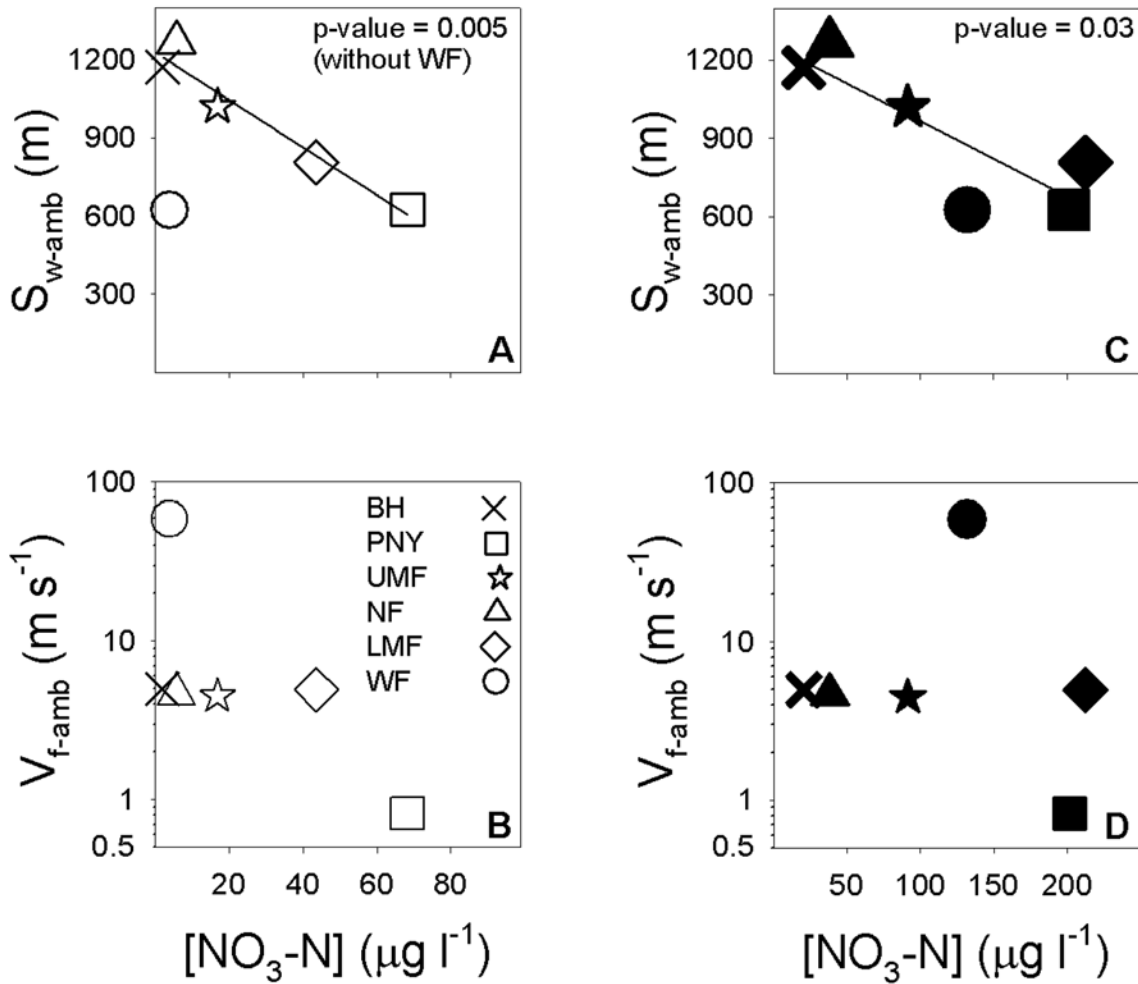


Figure 2.5: (A) Ambient uptake length ($S_{w\text{-amb}}$) and (B) ambient uptake velocity ($V_{f\text{-amb}}$) for the six stream reaches versus ambient $\text{NO}_3\text{-N}$ concentrations for the day of the experiment (open symbols). (C) Ambient uptake length ($S_{w\text{-amb}}$) and (D) ambient uptake velocity ($V_{f\text{-amb}}$) for the six stream reaches versus average annual $\text{NO}_3\text{-N}$ concentrations (solid symbols). (A) The relationship between ambient $\text{NO}_3\text{-N}$ concentrations and $S_{w\text{-amb}}$ was not significant for the six reaches ($p\text{-value} = 0.22$, $r^2 = 0.35$), but by excluding West Fork the relationship was significant for the other five reaches ($p\text{-value} = 0.005$, $r^2 = 0.95$). (C) The relationship between average annual $[\text{NO}_3\text{-N}]$ and $S_{w\text{-amb}}$ was significant for the six reaches ($p\text{-value} = 0.03$, $r^2 = 0.72$). (B) and (D) The relationships between $V_{f\text{-amb}}$ and both $[\text{NO}_3\text{-N}]$ ((B) ambient and (D) average annual) were not significant for the six reaches ($p\text{-value} = 0.42$ and 0.91 , $r^2 = 0.16$ and 0.003). Each symbol shape represents one of the six stream reaches: BH is Beehive, PNY is Pony, UMF is Upper Middle Fork, NF is North Fork, LMF is Lower Middle Fork, and WF is West Fork.

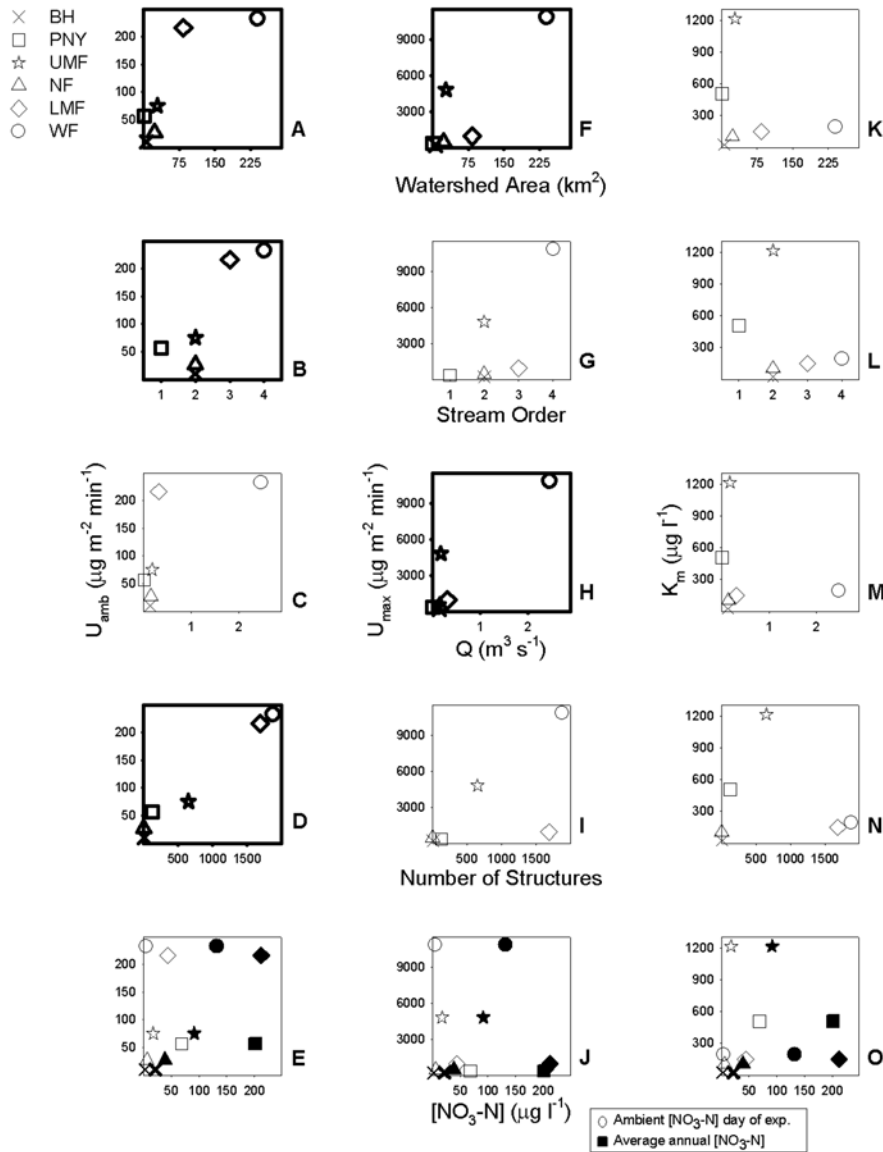


Figure 2.6: (A-E) Ambient areal uptake rate (U_{amb}), (F-J) maximum areal uptake rate (U_{max}), and (K-O) half-saturation constant (K_m), versus watershed area (WA), stream order, discharge (Q), number of structures, and NO_3 -N concentrations [NO_3 -N] (ambient for the day of the experiment (solid symbols) and average annual (open symbols)). Each symbol shape represents one of the six stream reaches: BH is Beehive, PNY is Pony, UMF is Upper Middle Fork, NF is North Fork, LMF is Lower Middle Fork, and WF is West Fork. A, B, D, F, and H have bold boundaries around the plots indicating each had a significant positive correlation (p -value ≤ 0.05): WA versus U_{amb} (A) yields a p -value = 0.03, $r^2 = 0.72$; stream order versus U_{amb} (B) yields a p -value = 0.04, $r^2 = 0.70$; number of structures versus U_{amb} (D) yields a p -value = 0.0001, $r^2 = 0.98$; WA versus U_{max} (F) yields a p -value = 0.02, $r^2 = 0.78$; Q versus U_{max} (H) yields a p -value = 0.01, $r^2 = 0.84$.

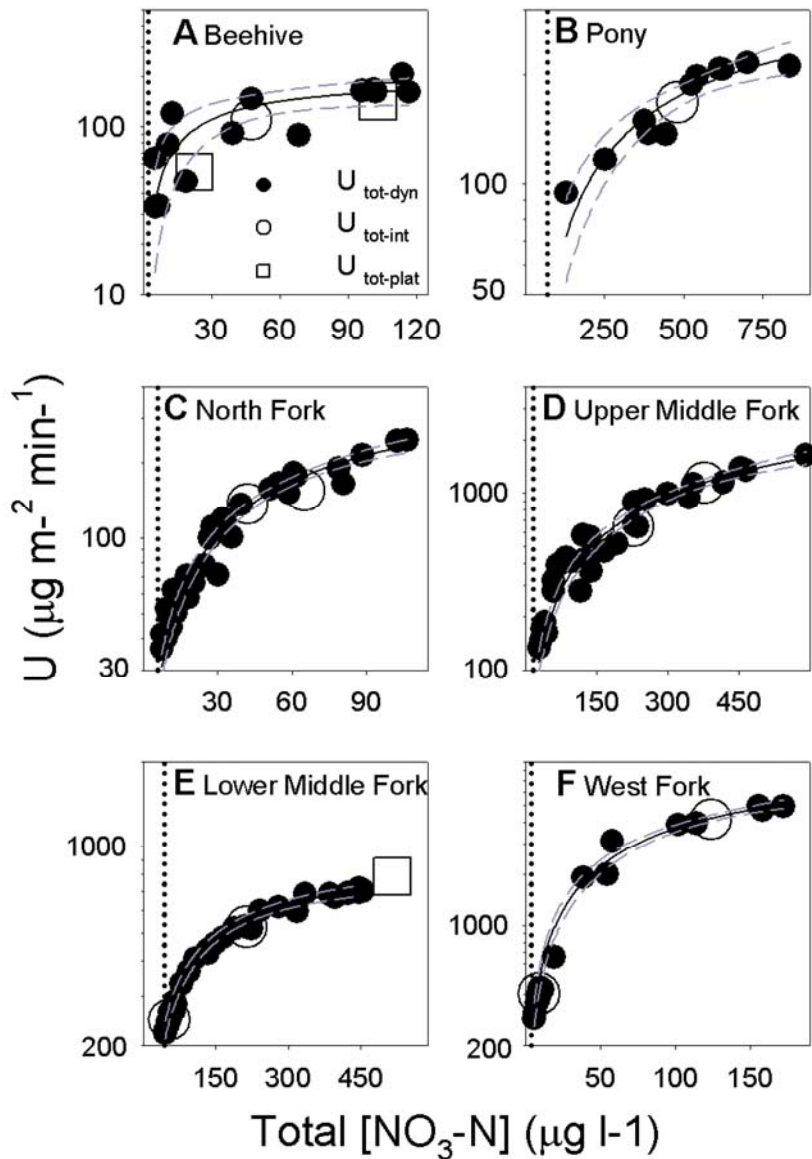


Figure 2.7: Total areal uptake rates of added nutrient plotted against total $\text{NO}_3\text{-N}$ concentration for six stream reaches. $U_{\text{tot-dyn}}$ is total areal uptake rate for each grab sample calculated using the dynamic TASC approach, $U_{\text{tot-int}}$ is total areal uptake rate calculated using the BTC-integrated approach, and $U_{\text{tot-plat}}$ is total areal uptake rate calculated using the plateau approach. Constant-rate tracer additions were only performed in Beehive (A) and Lower Middle Fork (E); these are the only sites with $U_{\text{tot-plat}}$ values. Michaelis-Menten hyperbolic equation fits (solid lines) with 95% confidence intervals (dashed lines) are shown for each experiment. (A-F) Vertical dotted lines on the left of the figure indicate ambient $\text{NO}_3\text{-N}$ concentrations for the day of the experiment. (A-F) Note the scale of the x and y-axes are different for each plot; they are modified to better show the data range and the M-M model fit for each experiment.

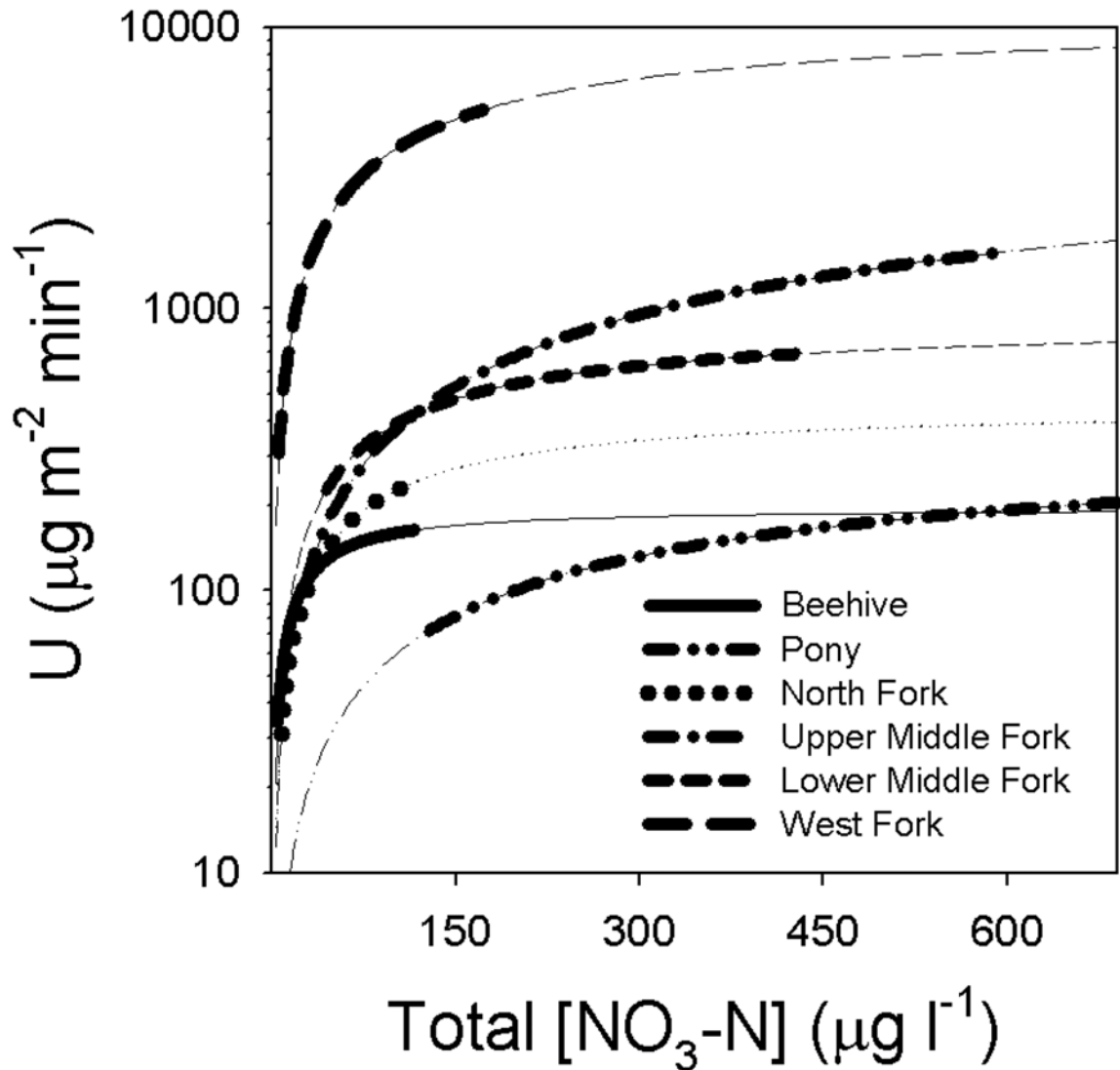


Figure 2.8: Michaelis-Menten (M-M) hyperbolic equation fits for total areal uptake rates for each grab sample calculated using the dynamic TASC approach ($U_{\text{tot-dyn}}$) versus total dynamic $\text{NO}_3\text{-N}$ concentration. The M-M models for this figure are the same data as Figure 2.7. This figure presents the data from the six sites on one graph and on the same axes for comparison and includes the models extended to the axes. The bold portions of the lines indicate the data range while non-bold sections indicate the extrapolation to the axes.

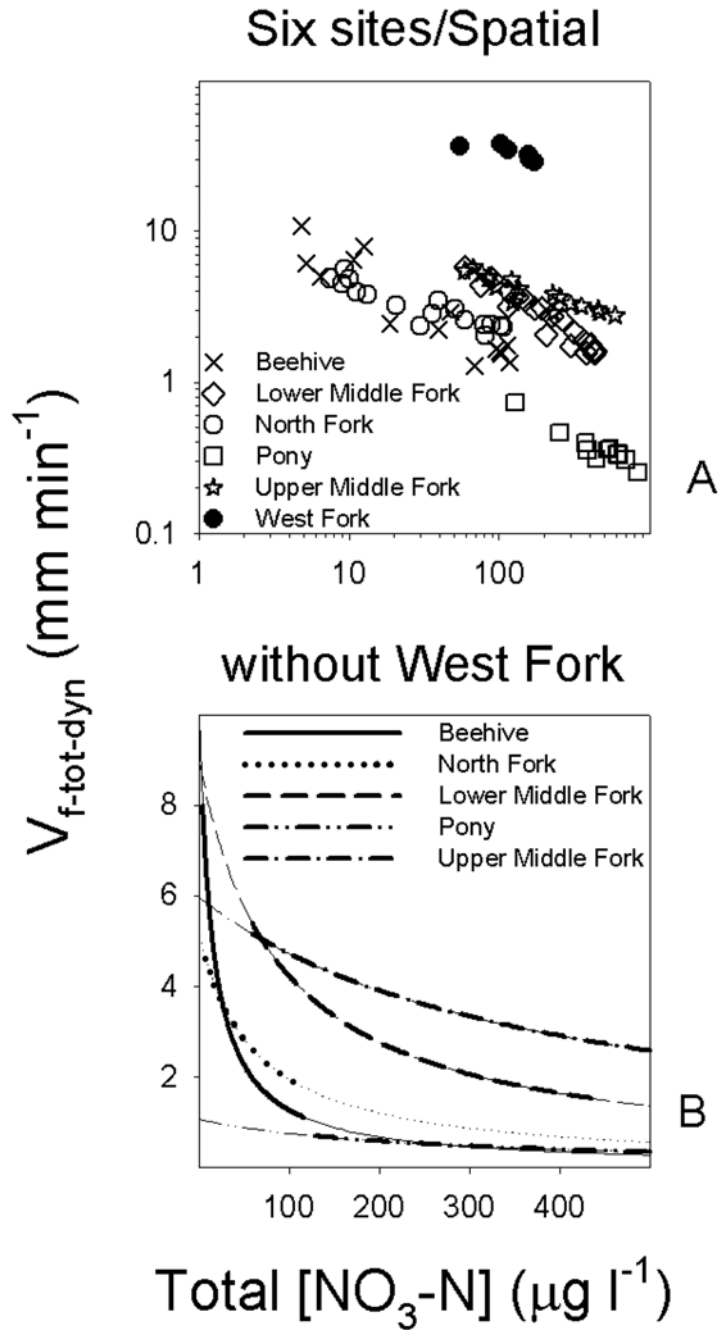


Figure 2.9: Total dynamic uptake velocities ($V_{f-tot-dyn}$) for each grab sample versus total dynamic $\text{NO}_3\text{-N}$ concentration $[\text{NO}_3\text{-N}_{tot-dyn}]$ for the six stream reaches (A). (B) For five of the six sites, the hyperbolic decay models for each data set are presented. (B) West Fork was excluded from the plot because the minimum $V_{f-tot-dyn}$ value for the $[\text{NO}_3\text{-N}_{tot-dyn}]$ range was more than twice as large as the largest $V_{f-tot-dyn}$ value for any of the other reaches. In (B), the bold portions of the lines indicate the fit for the data range and non-bold sections indicate an extrapolation to the axes.

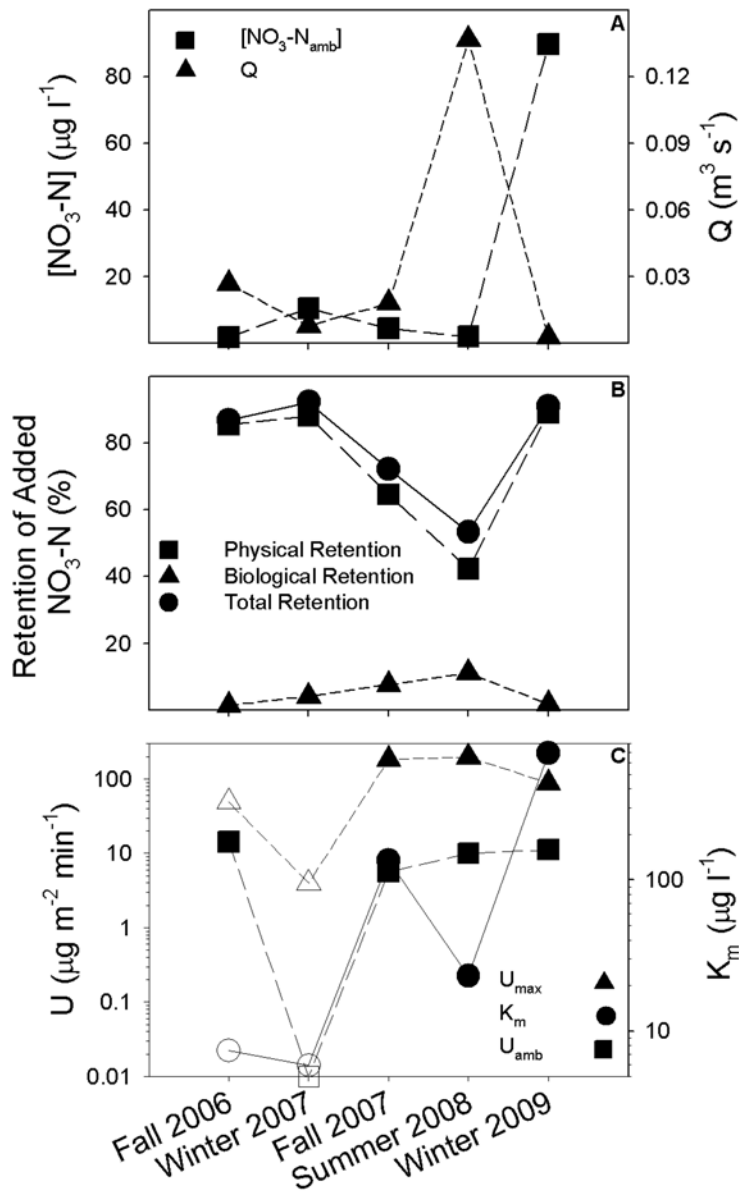


Figure 2.10: (A-C) Five tracer addition experiments were conducted in Beehive from fall 2006 to winter 2009. The same reach was used for each experiment. (A) Ambient $\text{NO}_3\text{-N}$ concentrations and discharge (Q) varied across seasons. (B) Seasonal total, physical and biological $\text{NO}_3\text{-N}$ retention. (C) Seasonal ambient areal uptake rate (U_{amb}), maximum areal uptake rate (U_{max}), and the half-saturation constant (K_m). Note that both y-axes are log scale. The open square for U_{amb} is for March 2007. When calculating the $S_{w\text{-amb}}$ for March 2007, the linear regression of $\text{NO}_3\text{-N}_{\text{tot-dyn}}$ concentration versus S_w yielded a negative y-intercept (negative $S_{w\text{-amb}}$) therefore, the U_{amb} was immeasurable. The filled symbols for U_{max} and K_m are the three experiments that yielded significant M-M model fits (p -values < 0.05). The symbols that are open yielded M-M model fits that were not significant (p -values > 0.05).

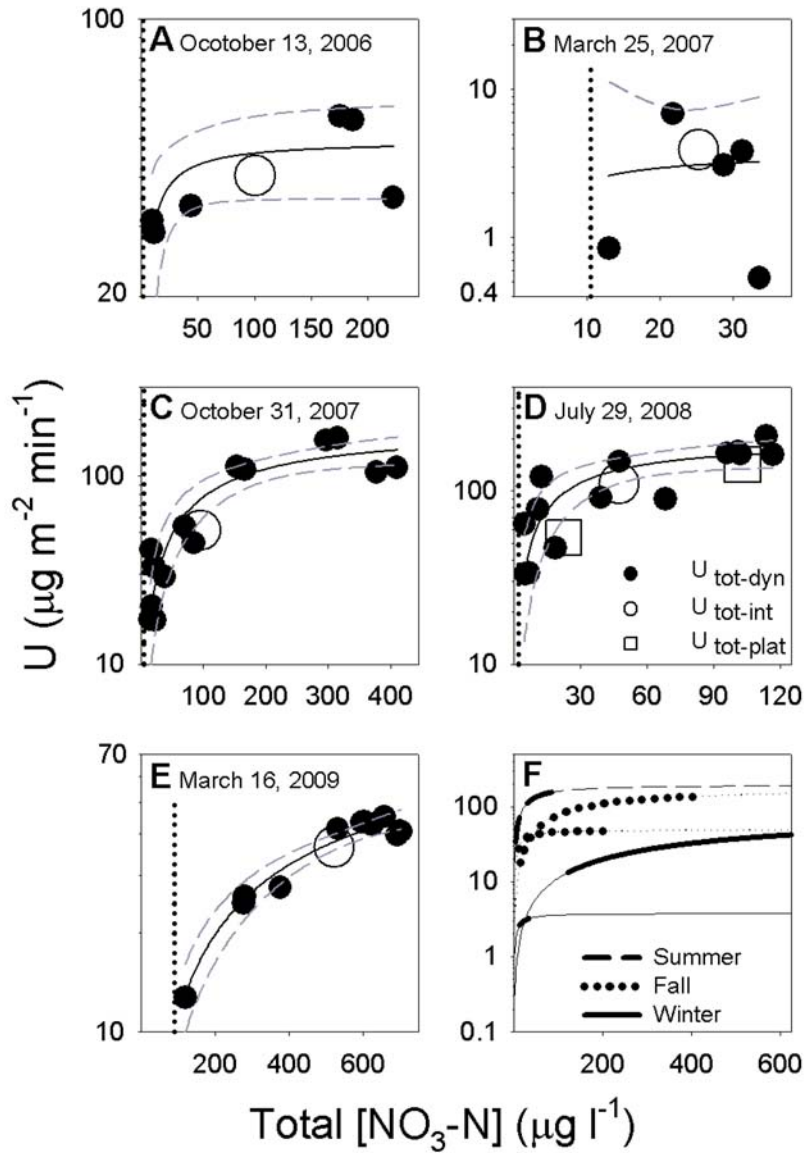


Figure 2.11: Total areal uptake rates versus total $\text{NO}_3\text{-N}$ concentrations in the Beehive experimental stream reach for five seasons. $U_{\text{tot-dyn}}$ is the total areal uptake rate for each grab sample calculated using the dynamic TASC approach, $U_{\text{tot-int}}$ is the total areal uptake rate calculated using the BTC-integrated approach, and $U_{\text{tot-plat}}$ is the total areal uptake rate calculated using the plateau approach. Constant-rate tracer additions were only performed in July 2008 (D); this is the only season with $U_{\text{tot-plat}}$ values. (A-E) Michaelis-Menten (M-M) hyperbolic models (solid lines) with 95% confidence intervals (dashed lines) are shown for each experiment. (A-E) Vertical dotted lines on the left of the figure indicate ambient stream $\text{NO}_3\text{-N}$ concentrations for the day of the experiment. (F) M-M fits compiled in one plot, the bold portions of the lines indicate the model fits for the data range and non-bolded sections indicate the extrapolation to the axes. (A-F) Note the scale of the x and y-axes is different for each plot; they are modified to better show the data range and the M-M model fit for each experiment.

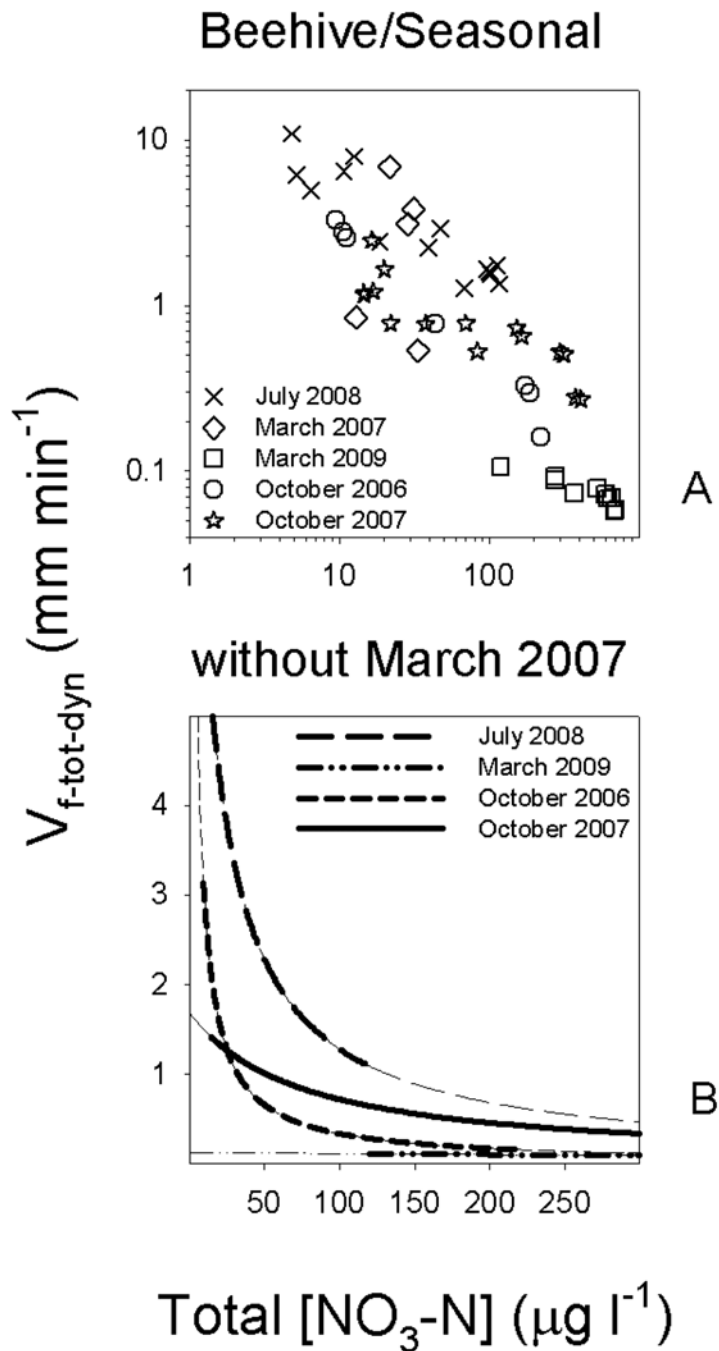


Figure 2.12: Total dynamic uptake velocities ($V_{f\text{-tot-dyn}}$) for each grab sample versus total dynamic $\text{NO}_3\text{-N}$ concentration [$\text{NO}_3\text{-N}_{\text{tot-dyn}}$] for the five seasonal experiments in Beehive (A). (B) For four of the five seasons, the hyperbolic decay model fit for each data set is presented. (B) March 2007 was excluded because the hyperbolic decay model fit was not significant (p -value is 0.9743). In (B), the bold portions of the lines indicate the fit for the data range and non-bolded sections indicate an extrapolation to the axes.

CHAPTER 3

SUMMARY

Increased stream water nitrate concentration has coincided with increased development over the last four decades in the West Fork Gallatin Watershed and has modified the streams network's capacity to retain nitrate. We sought to determine if increased in-stream nitrate has changed retention and uptake kinetics across varying development intensities within the 240 km² watershed and across seasons.

Through this research we found:

(1) *Varying development intensities and scale affected stream nitrate uptake kinetics and spiraling parameters.* Past studies have shown that major influencing drivers for stream uptake are discharge (Valett et al. 1996, Butturini and Sabater 1998) and ambient nutrient concentrations (Mulholland et al. 2008). We found a general decrease in ambient uptake lengths with increasing nitrate concentrations across the watershed; this is not consistent with the paradigm that S_{w-amb} generally increases with increasing nitrate concentrations. While ambient and maximum areal uptake rates both increased with larger watershed area, neither of them showed strong correlation with nitrate concentrations. Our results imply that the factors driving uptake kinetics are too complex to use one driving factor to predict uptake kinetics, rather utilizing a combination of factors (i.e., including but not limited to: biological community assemblage, metabolism, nutrient stoichiometry, light availability, antecedent nutrient

dynamics, and hydrologic setting) should be employed to better predict how a stream reach or network will respond to increases in development intensity and nutrient loading.

(2) *Nitrate uptake kinetics and spiraling parameters varied across seasons in Beehive (one of the six stream experimental reaches within the watershed), a snow dominated mountain stream.* Although U_{amb} did not vary widely across seasons, both U_{max} and K_m varied. Relatively consistent U_{amb} values across seasons implicate that uptake occurs year round and varying U_{max} and K_m values suggest that capacity for uptake of elevated nitrate varies across seasons. Highest U_{max} values and lowest K_m values occurring during summer indicates the stream has a more rapid response and greater capacity for increased nitrate retention.

(3) *Scale was a main driver of retention of added nitrate across the West Fork Gallatin Watershed.* Across the stream network, as watershed area increased, physical retention of added nitrate decreased and biological retention of added nitrate increased. Across seasons, the highest ratio of biological to total retention of added nitrate occurred during summer indicating increased biological uptake during this time period, but physical retention comprised the larger proportion of total retention of added nitrate throughout the year.

This research provides insight to nutrient spiraling in streams across a stream network with varying development intensities. To continue to improve understanding of stream network nutrient retention and uptake potential, more research quantifying nutrient retention from ambient to saturated conditions over space, time, and development intensities is required. Further, results from this study highlight the need to

consider both physical and biological processes occurring in streams for understanding the capacity of stream networks to buffer nutrient loading and downstream export.

Results from this research provide insight into the saturation state of streams in the West Fork Watershed and indicate change from undeveloped conditions. The methods and analyses presented in this thesis are applicable across other ecosystems as stream nutrient state assessment tools and could help future quantification of stream ecosystems and highlight shifts in ecosystem dynamics in response to increased nutrient loading.

References Cited

- Butturini, A. and F. Sabater. 1998. Ammonium and phosphate retention in a Mediterranean stream: hydrological versus temperature control. *Canadian Journal of Fisheries and Aquatic Sciences* **55**:1938-1945.
- Mulholland, P. J., A. M. Helton, G. C. Poole, R. O. Hall, S. K. Hamilton, B. J. Peterson, J. L. Tank, L. R. Ashkenas, L. W. Cooper, C. N. Dahm, W. K. Dodds, S. E. G. Findlay, S. V. Gregory, N. B. Grimm, S. L. Johnson, W. H. McDowell, J. L. Meyer, H. M. Valett, J. R. Webster, C. P. Arango, J. J. Beaulieu, M. J. Bernot, A. J. Burgin, C. L. Crenshaw, L. T. Johnson, B. R. Niederlehner, J. M. O'Brien, J. D. Potter, R. W. Sheibley, D. J. Sobota, and S. M. Thomas. 2008. Stream denitrification across biomes and its response to anthropogenic nitrate loading. *Nature* **452**:202-U246.
- Valett, H. M., J. A. Morrice, C. N. Dahm, and M. E. Campana. 1996. Parent lithology, surface-groundwater exchange, and nitrate retention in headwater streams. *Limnology and Oceanography* **41**:333-345.